

SERPENTINE TEXTURES AND SERPENTINIZATION

F. J. WICKS

Department of Mineralogy and Geology, Royal Ontario Museum, Toronto, Canada M5S 2C6

E. J. W. WHITTAKER

Department of Geology and Mineralogy, Oxford University, Oxford, England OX1 3PR

ABSTRACT

Textures of serpentines observed in thin section can be divided into three types: pseudomorphic textures formed after olivine, pyroxene, amphibole, talc and chlorite; non-pseudomorphic textures formed either from the same primary minerals or from pseudomorphic serpentine textures; and textures formed in serpentine veins. Microbeam X-ray camera results indicate that the pseudomorphic textures (mesh texture after olivine, and bastites after pyroxene, amphibole etc.) are most commonly composed of lizardite $1T \pm$ magnetite or lizardite $1T +$ brucite \pm magnetite. Antigorite or chrysotile $2M_{c1} \pm$ magnetite, or antigorite or chrysotile $2M_{c1} +$ brucite \pm magnetite pseudomorphic textures occur infrequently. Non-pseudomorphic interpenetrating and interlocking textures are most commonly composed of antigorite \pm magnetite, but antigorite $+ brucite \pm magnetite$ and chrysotile $2M_{c1}$ and/or lizardite $1T \pm brucite \pm magnetite$ also occur.

Hourglass textures of α -serpentine and mesh textures with α -serpentine mesh rims and α , γ or isotropic serpentine mesh centers, and bastites of α - or γ -serpentine are mainly lizardite $1T$ or lizardite $1T +$ brucite. The brucite occurs as a fine intergrowth with lizardite and is optically indistinguishable from it. Interpenetration and interlocking textures of γ -serpentine are usually antigorite, but in some cases it is not possible to distinguish chrysotile, lizardite and antigorite in non-pseudomorphic textures without X-ray evidence. Brucite, however, occurs in discrete grains in non-pseudomorphic textures and is easily identified. Interlocking textures of α -serpentine are usually lizardite, often a multi-layer polytype, but some are composed of intimate mixtures of lizardite $1T$ and chrysotile $2M_{c1}$. Antigorite and chrysotile asbestos can be recognized in veins, but non-fibrous chrysotile and lizardite are optically indistinguishable.

Serpentinization processes are divided into eight types depending on whether the conditions involve, or do not involve, rising temperatures, presence of substantial shear, and nucleation of antigorite. Three main regimes of temperature are recognized which correspond to the stability of different serpentine mineral and brucite assemblages. These categories permit a systematization of the various textures and mineral assemblages, the redox conditions during serpentinization, and the conditions requisite for the formation of chrysotile asbestos deposits.

SOMMAIRE

La texture des serpentines, telle qu'on l'observe en lames minces, est de trois types: (1) texture pseudomorphe d'olivine, pyroxène, amphibole, talc et chlorite; (2) texture non-pseudomorphe formée à partir des mêmes minéraux primaires ou bien d'une texture pseudomorphe déjà en place; (3) texture formée dans un filon de serpentine. D'après l'analyse à la chambre aux rayons X à micro-faisceau, les textures pseudomorphes (texture réticulée héritée de l'olivine; bastites provenant de pyroxène, d'amphibole, . . .) se composent le plus souvent de lizardite $1T \pm$ magnétite ou de lizardite $1T +$ brucite \pm magnétite. Comme textures pseudomorphes peu fréquentes, citons: antigorite ou chrysotile $2M_{c1} \pm$ magnétite; antigorite ou chrysotile $2M_{c1} +$ brucite \pm magnétite. Les textures non-pseudomorphes, avec interpénétration et enchevêtrement, consistent surtout en antigorite \pm magnétite; parfois en antigorite $+ brucite \pm magnétite$, ou encore chrysotile $2M_{c1}$ ou lizardite (ou les deux) $\pm brucite \pm magnétite$. Les textures en sablier de serpentine α et les textures réticulées où le centre est fait de serpentine α , γ ou isotrope et la périphérie est faite de serpentine α , ainsi que les bastites de serpentines α ou γ , se composent principalement de lizardite $1T$ avec ou sans brucite. La brucite se présente en intercroissance intime avec la lizardite, dont on ne peut la distinguer optiquement. Les textures de serpentine γ à interpénétration et enchevêtrement sont d'ordinaire de l'antigorite, mais dans certains cas on ne peut distinguer entre chrysotile, lizardite et antigorite dans les textures non-pseudomorphes sans le secours des rayons X. La brucite, par contre, se présente en grains bien séparés et facilement identifiables dans ces textures. Les textures à enchevêtrement de serpentine α sont d'ordinaire de la lizardite, souvent polytype à couches multiples, mais certaines d'entre elles sont constituées de lizardite $1T$ et de chrysotile $2M_{c1}$ intimement mélangés. On peut reconnaître l'antigorite et le chrysotile dans les filons d'asbeste, mais le chrysotile fibreux et la lizardite ne se distinguent pas optiquement.

Les processus de serpentinisation se divisent en huit types, selon qu'ils impliquent ou non: (1) accroissement de température, (2) glissements notables, (3) nucléation d'antigorite. On distingue trois régimes de température, qui correspondent à la stabilité des différents assemblages des minéraux de serpentine et de brucite. Ces catégories permettent de systéma-

tiser les diverses textures et les assemblages de minéraux, les conditions rédox au cours de la serpentinisation et les conditions requises pour la formation de gîtes d'asbeste-chrysotile.

(Traduit par la Rédaction)

INTRODUCTION

Some data are available on the mineralogy of the textures in serpentinized ultramafic rocks. X-ray powder-diffraction studies of bulk samples, serpentine concentrates, or material hand picked from thin sections (Hochstetter 1965) have indicated that mesh texture and bastite assemblages are composed mainly of various combinations of lizardite, chrysotile and brucite (Green 1961; Hochstetter 1965; Coleman 1966; Page 1967a, 1968; Aumento 1970; Boudier 1971; Coleman & Keith 1971), and that thorn or flame textures are composed mainly of antigorite (Green 1961; Hochstetter 1965; Boudier 1971). X-ray powder-diffraction studies of bastites picked from hand specimens or thin sections (Whittaker & Zussman 1956; Hochstetter 1965), or drilled from polished sections (Page 1967a) indicate that most bastites are composed of lizardite, and a few of chrysotile. These results contradict the suggestion of Winchell & Winchell (1959) and Hess *et al.* (1952) that bastites consist of antigorite, although Hochstetter (1965) and Boudier (1971) have identified some possible antigorite bastites as well as lizardite bastites.

Most of these identification techniques are limited by the fact that the optical properties of the mineral fragments cannot be related, with certainty, to the variety of optical properties observed within the different textural units. Hochstetter (1965) partly overcame this problem by removing fragments with specific textures from thin section under the polarizing microscope and mounting each fragment in a Debye-Scherrer camera. However, this method is limited by the relatively large size of the fragment, about 0.5×0.3 mm, in respect to the size of the various textural units (for example, mesh rims range from 0.01 to 0.30 mm and average 0.07 mm - Wicks *et al.* 1977). The Norelco-type microbeam X-ray diffraction camera, used in the present study, overcomes these difficulties. The camera accommodates a fragment of thin section up to 10×10 mm, and textural units within the fragment can be aligned with the 50 mm diameter Pb-glass collimator under a petrographic microscope (Wicks & Zussman 1975).

The serpentine mineral textures can be divided into three groups: pseudomorphic textures and non-pseudomorphic textures, both of which form by the replacement of pre-existing min-

erals, and vein textures which form by crystallization in fractures. It is the purpose of this paper (1) to describe the serpentine textures and identify the component minerals, (2) to establish criteria for the optical identification of the serpentine minerals in these textures, and (3) to discuss the conditions of formation of the serpentine minerals and textures.

EXPERIMENTAL METHODS

The Norelco-type microbeam X-ray diffraction camera was used for *in situ* textural studies following the procedure outlined in Wicks & Zussman (1975). Supplementary data were obtained from 114.6 mm diameter powder-diffraction cameras using Ni-filtered Cu radiation. The material for these diffraction patterns was either picked from thin section (areas down to 0.5×0.5 mm) or removed from hand specimens, ground in acetone, and mounted in 0.2 mm diameter glass capillaries. Fibrous and splintery serpentine bundles were subjected to X-ray examination in 60 mm diameter Unicam oscillation-rotation cameras using Ni-filtered Cu radiation, and both stationary and rotated specimens.

Thin sections of 1300 serpentinized and partly serpentinized ultramafic rocks from various locations were examined. From these, 79 were selected as representative of the various textures and studied with the microbeam X-ray camera. The results are presented in Tables 1, 2, and 3. Each Table is divided according to the type of serpentinization represented. These types, numbered 1 to 8, are defined later in this paper, but it is necessary to refer to them in advance of their definition in order to locate particular entries in the Table. The types are further subdivided into various geological environments, although the serpentinized ultramafic rocks may or may not be at the same metamorphic grade as the country rocks.

PSEUDOMORPHIC TEXTURES

Pseudomorphic textures form through the serpentinization of almost all minerals in ultramafic rocks. The perfection of pseudomorphism varies from excellent to indistinct, and the latter grade into non-pseudomorphic textures. Many massive serpentinites are composed of pseudomorphic textures, but most of the associated foliated serpentinites are composed of non-pseudomorphic textures as is discussed in the following sections.

Olivine

Olivine alters along fractures and grain boun-

daries to form easily recognized pseudomorphs composed of mesh and hourglass textures. Either may be composed of α - or γ -serpentine. A detailed discussion of the form of these textures, with several figures, has been given in Wicks, Whittaker and Zussman (1977). Frequent refer-

ence is made to these figures, and for brevity they are denoted as WWZ followed by the Figure number. Forty-four α -serpentine mesh textures, four α -serpentine pure hourglass textures, five γ -serpentine mesh textures, and five γ -serpentine pure hourglass textures were examined

TABLE 1. X-RAY RESULTS ON PSEUDOMORPHIC TEXTURES FROM VARIOUS ULTRAMAFIC BODIES

Location	Sample No.	Texture	Location	Sample No.	Texture
<u>TYPE 1 SERPENTINIZATION</u>					
ANTIGORITE \pm MAGNETITE			LIZARDITE 1γ + BRUCITE \pm MAGNETITE		
<i>stratiform intrusions</i>			<i>stratiform intrusions</i>		
Fox River, Manitoba	FW-FR-1	γ -mesh	Muskox, N.W.T.	18482	α -mesh [†]
				18483	α -mesh
<u>TYPE 3 SERPENTINIZATION</u>			<i>concentrically zoned intrusions</i>		
LIZARDITE 1γ \pm MAGNETITE			<i>alpine-type intrusions</i>		
<i>stratiform intrusions</i>			<i>alpine-type intrusions</i>		
Stillwater, Montana	18477	α -mesh	Glen Urquhart, Scot.	18508	α -mesh, γ -tal α -bast
	18478	α -mesh, plag	Kaponigbach, Austria	18525	α -mesh
	18479	α -mesh, γ - α -cpx-bast	Mayaguez, Puerto Rico	18529	α -mesh, γ -opx-bast **
	18480	γ - α -is-opx-bast	Jeffrey mine, Quebec	18541	α -mesh [†]
Muskox, N.W.T.	18484	α -mesh	Mount Albert, Quebec	18549	α -mesh, γ - α -opx-bast
Fox River, Manitoba	18485	α -mesh		18550	α -mesh, γ - α -opx + α - γ -amp-bast **
	FW-FR-1	α -mesh		18552	γ -opx-bast **
<i>differentiated sills</i>				18553	α -mesh, γ - α -opx-bast
Quill Creek, Yukon	18487	α -mesh		18562	α -mesh, α - γ -amp-bast **
Tadamagouche Creek, Yukon	1867-249	γ -mesh		18564	α -mesh, α - γ -amp-bast **
Telson Lake, Yukon	1867-265	γ -mesh	Pinchi Lake, B.C.	18554	α -mesh, γ -opx-bast **
<i>alpine-type intrusions</i>			<u>TYPE 5 SERPENTINIZATION</u>		
Glen Urquhart, Scotland	18509	α -mesh, α - γ -is-amp-bast	CHRYSOTILE + BRUCITE \pm MAGNETITE		
Lizard, England	18510	α -mesh, γ -opx-bast, γ -chl-bast	<i>alpine-type intrusions</i>		
	18511	α -mesh, γ -opx-bast	<i>alpine-type intrusions</i>		
	18512	α -mesh	Jeffrey mine, Quebec	18538	γ -hgls ^P
	18513	α -mesh		18541	γ -hgls
	18514	α -mesh	LIZARDITE 1γ + CHRYSOTILE 2H_{a1} \pm MAGNETITE		
	18516	α -mesh	<i>Precambrian high-grade metamorphic terrain</i>		
Kaponigbach, Austria	18524 [†]	α -mesh, γ - α -opx? * -bast	<i>Pipe Lake mine, Man.</i>		
Totalp, Davos, Switzerland	18527	α -mesh, γ -opx-bast	18500	α -hgls, α - γ -cpx?-bast	
Mayaguez, Puerto Rico	18528 [†]	α -mesh, γ -opx-bast	18501	γ -mesh	
	18530	α -mesh, γ - α -opx?-bast	<u>TYPE 7 SERPENTINIZATION</u>		
Jeffrey mine, Quebec	18538	α -mesh, α -opx?-bast	ANTIGORITE \pm MAGNETITE		
	18540	α -hgls, γ -opx?-bast	<i>stratiform intrusions</i>		
Mount Albert, Quebec	18551	α -mesh	<i>Stillwater, Montana</i>		
Shulap Range, B.C.	18556	α -mesh, γ -opx-bast	18481 γ -hgls		
Branganca, Portugal	18563	α -mesh	<i>Precambrian high-grade metamorphic terrain</i>		
<i>Precambrian high-grade metamorphic terrain</i>			<i>Oswagan Lake, Man.</i>		
Bowden Lake, Manitoba	18489	α -mesh	18498 γ -hgls, γ -chl-bast		
	18490	α -mesh, γ -phl-bast	<i>Precambrian low-grade metamorphic terrain</i>		
Bucko Lake, Manitoba	18492	α -mesh	<i>Knee Lake, Man.</i>		
Joey Lake, Manitoba	18493	α -hgls	18558 γ -hgls		
Little Clarke Lake, Man.	18494	α -mesh	ANTIGORITE + BRUCITE \pm MAGNETITE		
	18495	α -mesh [†]	<i>alpine-type intrusions</i>		
Moak Lake, Manitoba	18497	α -mesh	<i>Jeffrey mine, Quebec</i>		
Pipe Lake mine, Manitoba	18499	α -mesh, γ - α -opx?-bast	18544 γ -mesh		
Setting Lake, Manitoba	18503	α -mesh, γ -opx?-bast			
	18505	α -mesh, γ -chl-bast			
	18506	α -mesh [†]			
<i>Precambrian low-grade metamorphic terrain</i>					
Island Lake, Manitoba	18557	α -mesh			

18000 series = Oxford University accession numbers; FW series = F.J. Wicks field numbers; IB67 = T.N. Irvine, Geological Survey of Canada numbers.

α = α -serpentine; γ = γ -serpentine; is = isotropic; mesh = mesh texture; hgls = pure hourglass texture; bast = bastite; opx = orthopyroxene; cpx = clinopyroxene; amp = amphibole; chl = chlorite; phl = phlogopite; plag = plagioclase.

B.C. = British Columbia; Man. = Manitoba; N.W.T. = Northwest Territories; Scot. = Scotland.

*The ? indicates that the exact nature of the pre-serpentinization mineral is uncertain.

**These bastites are composed of lizardite 1 γ + brucite. All the other bastites are composed of lizardite 1 γ only.

†Indication of 2 H polytypes in some microbeam diffraction patterns.

^PPovlen-type chrysotile

with a total of 371 X-ray microbeam camera exposures (Table 1).

The most common accessory mineral produced by the serpentinization of olivine is mag-

netite. There is often a correlation between the distribution of the magnetite and both the degree of serpentinization and the color of the serpentinite. In the early stages, magnetite forms

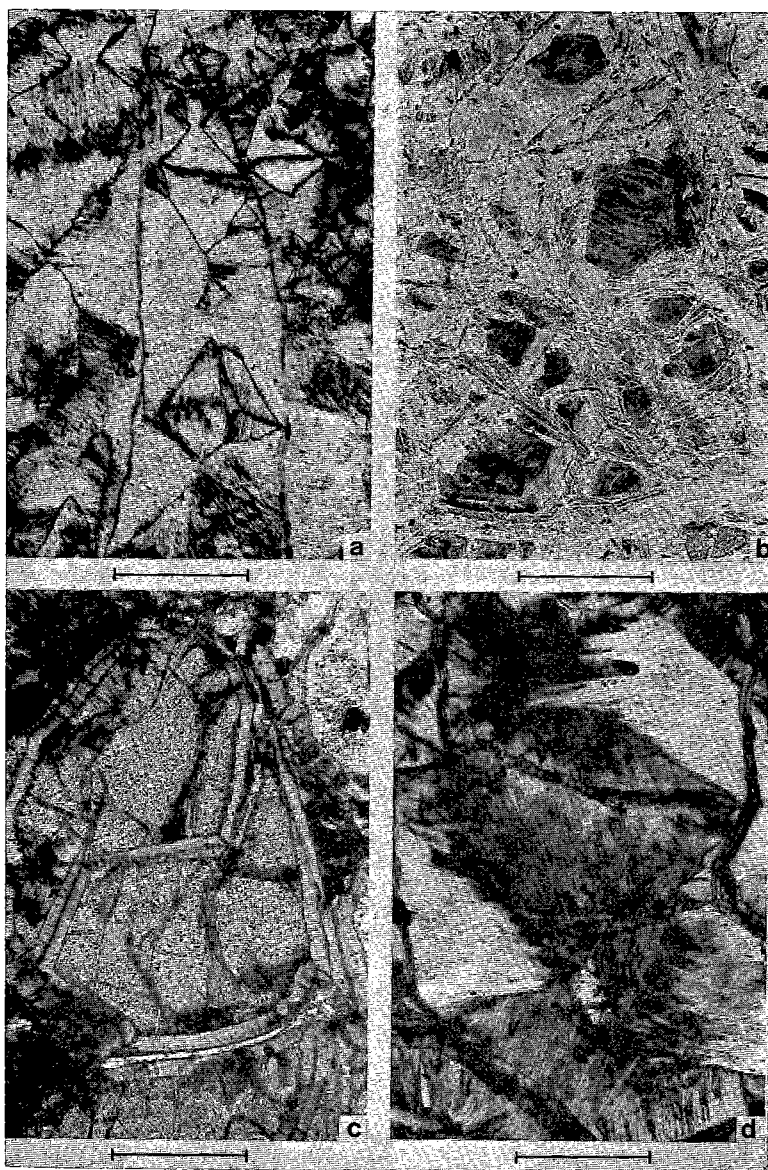


FIG. 1. (a) Lizardite 1T (α -serpentine) pure hourglass texture. Sample 18540, Jeffrey mine, Quebec. (b) Lizardite 1T + brucite mesh texture, mesh rims of lizardite (α -serpentine) with minor brucite, and reddish brown mesh centers of an intimate mixture of brucite and minor lizardite. Plain polarized light. Sample 18529, Mayaguez, Puerto Rico. (c) Lizardite 1T (γ -serpentine) mesh rims with relict olivine mesh centers. Sample IB67-249, Telson Lake, Yukon. (d) Chrysotile $2M_{c1}$ and $2O_{r1}$ (γ -serpentine) pure hourglass texture with anhedral brucite grains towards center of one hourglass unit. Sample 18538, Jeffrey mine, Quebec. All except (b) under crossed nicols. Bar represents 0.2 mm.

very fine discrete grains distributed throughout the serpentine, and the rock is black or dark grey. As serpentinization progresses the magnetite forms coarser grains and concentrates in mesh centers or in the central parting of mesh rims, and the rock is usually a pale gray or brown. At later stages the magnetite migrates out of the mesh or hourglass textural units into cross-cutting lenses and veinlets, and the rock is usually green, often a pale green.

α -serpentine mesh and hourglass textures. The α -serpentine mesh textures (Type 3, Table 1 and WWZ Fig. 1) and hourglass textures (mainly Type 3, Table 1 and Fig. 1a) were found to be composed mainly of lizardite 1T, although approximately one microbeam diffraction pattern in 40 contained weak extra reflections suggesting the presence of some lizardite 2H. One of the pure hourglass texture specimens (18500, Type 5, Table 1) contained very minor amounts of chrysotile $2M_{c1}$ in intimate association with lizardite 1T. The lizardite in the mesh rims and hourglass textural units often occurs as "apparent fibers" lying at a high angle to the original fracture in the olivine (WWZ Figs. 2a, d). In other cases the lizardite does not appear to be fibrous so that mesh rims appear as two lizardite plates lying on either side of the central fracture (WWZ Fig. 1a). In all cases the lizardite yields microbeam diffraction patterns with z approximately parallel to α and the "apparent fiber" axis, and elements of x and y parallel to γ (Figs. 6g, h in Wicks & Zussman 1975).

Eleven of the mesh textures and one of the pure hourglass textures also contain brucite in an intimate submicroscopic mixture with the lizardite (Fig. 6f in Wicks & Zussman 1975). The brucite in the mesh rims (WWZ Fig. 1b) and hourglass textures is aligned with the z axis parallel to the z axis of lizardite. In general, the microbeam diffraction patterns from mesh rims, with or without brucite, show better orientation than those from hourglass textures.

Serpentine mesh centers generally were found to be composed of lizardite 1T \pm brucite regardless of the optical character of the centers. Exceptions occur where lizardite mesh centers or relict olivine mesh centers were replaced by chrysotile, antigorite, or 6-layer lizardite, during later development of non-pseudomorphic textures. These exceptions will be described in the section on Intermediate Textures. The lizardite \pm brucite in the α - and γ -serpentine mesh centers often has an average z -axis direction parallel to that of the lizardite (α -serpentine) in the adjacent mesh rims, but has less preferred orientation. The average z -axis direction always coincides

with the α -ray. Isotropic serpentine (serpophite) mesh centers (WWZ Fig. 1b) usually yield a randomly oriented lizardite diffraction pattern (Fig. 6j in Wicks & Zussman 1975) and only rarely a diffraction pattern with the z axis parallel to the X-ray beam (Fig. 6f in Wicks & Zussman 1975). The infrequent occurrence of the latter is explained in the discussion of idealized textures by Wicks *et al.* (1977).

Microbeam diffraction lines are commonly broader for lizardite mesh centers than for the associated lizardite mesh rims (compare Fig. 6j and 6g in Wicks & Zussman 1975). This suggests that the lizardite in mesh centers is finer grained and/or more poorly crystallized than that in mesh rims. It may be that minor chrysotile $2M_{c1}$ occurs intimately associated with the lizardite 1T in the mesh centers (Cressey & Zussman 1976), but is not detected because of the diffuse nature of the 20 l and 13 l reflections on the microbeam diffraction patterns.

Brucite, both in mesh rims and centers, is variable with locality and even within individual specimens, but there is rarely any visual indication of its presence. Brucite and magnetite coexist in thin section and their amounts are commonly in an inverse relationship. A few brucite-bearing textural units (Fig. 1b) are characterized by a reddish brown color, often called "iddingsite" or "bowlingite" (Francis 1956; Mattson 1964), but not all reddish-brown areas contain brucite.

γ -serpentine mesh and hourglass textures. Of the five specimens with γ -serpentine mesh texture, two have mesh rims of antigorite (FW-FR-1, Type 1 and 18544, Type 7, Table 1), two of lizardite (IB67-249, IB67-265, Type 3, and Fig. 1c) and one of chrysotile $2M_{c1}$ (18501, Type 5). Three of these have mesh centers of olivine. The fourth, with antigorite mesh rims, (FW-FR-1, Type 1) has later-formed secondary rims and mesh centers of lizardite (WWZ Fig. 2b). The fifth specimen, with chrysotile $2M_{c1}$ mesh rims (18501, Type 5), has mesh centers composed of a mixture of chrysotile $2M_{c1}$ and lizardite 1T, (WWZ Fig. 2c). Of the five specimens with γ -serpentine hourglass textures, three are antigorite (18481, 18498, 18558, Type 7, and WWZ Fig. 3a), and two are chrysotile ($2M_{c1}$ and $2Or_{c1}$) with brucite (18538, 18541, Type 5, and Fig. 1d).

The antigorite occurs as blades, or less frequently as apparent fibers, and yields antigorite microbeam diffraction patterns with y approximately parallel to γ and elements of x and z approximately parallel to α (Figs. 6o,p in Wicks & Zussman 1975). The lizardite also occurs as

blades or very fine apparent fibers (Fig. 1c) but yields lizardite $1T$ microbeam patterns with elements of x and y approximately parallel to γ and z approximately parallel to α . The chrysotile oc-

curs as fibers (Fig. 1d) or apparent blades, and yields chrysotile $2M_{c1}$ microbeam patterns that may (Fig. 6b in Wicks & Zussman 1975) or may not have associated chrysotile $2Or_{c1}$ or, less fre-

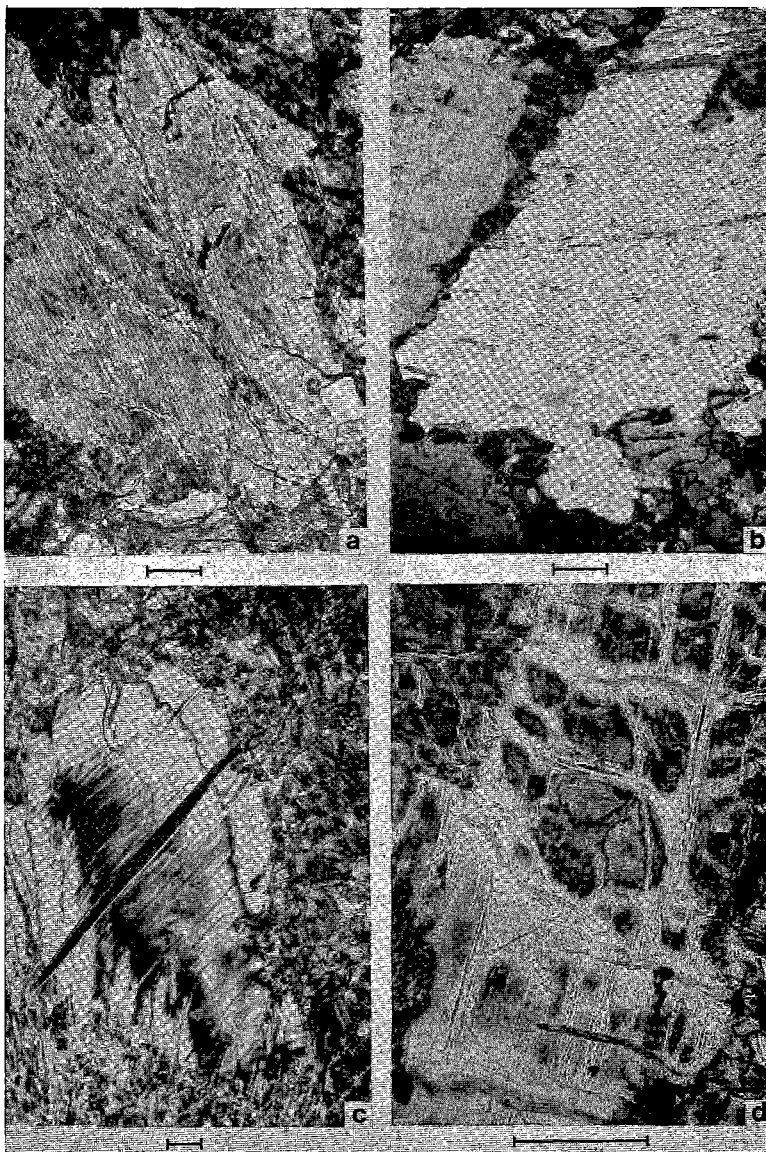


FIG. 2. (a) Lizardite $1T$ (γ -serpentine apparent fibers) bastite after orthopyroxene. Sample 18528, Mayaguez, Puerto Rico. (b) Lizardite $1T$ bastite, after orthopyroxene, as a nearly featureless plate. Sample 18540, Jeffrey mine, Quebec. (c) A complex lizardite $1T$ bastite after orthopyroxene with a marginal zone of α -serpentine and an inner core of γ -serpentine. Sample 18538, Jeffrey mine, Quebec. (d) Lizardite $1T$ bastite after orthopyroxene as a type of "mesh texture" with γ -serpentine apparent fiber rims surrounding α -serpentine apparent fiber centers. Sample 18527, Davos, Switzerland. All under crossed nicols. Bar represents 0.2 mm.

quently, parachrysotile (Fig. 6a in Wicks & Zussman 1975). The chrysotiles have x approximately parallel to γ , and y and z approximately parallel to α ; parachrysotile has y approximately parallel to γ , and x and z approximately parallel to α . Some diffraction patterns have extra reflections, outside that of the (130), which can be rationally indexed (Fig. 6b in Wicks & Zussman 1975) and identified as those of Povlentye chrysotile (Krstanović & Pavlović 1964; Middleton & Whittaker 1976; Cressey & Zussman 1976).

Pyroxenes

Serpentine pseudomorphs after pyroxenes are generally called bastites, a term of long standing in the literature (Haidinger 1845). The term has also been applied to serpentine pseudomorphs after amphiboles (Weigand 1875; Rost 1959; Klinkhammer 1962; Hochstetter 1965). Hochstetter (1965) has pointed out that, once serpentinization is complete, it is often impossible to distinguish a pyroxene bastite from an amphibole bastite. We have found that serpentinization of talc, chlorite and phlogopite also produces bastites indistinguishable from those after chain silicates. Therefore, it seems preferable to use the term for a serpentine pseudomorph after chain or sheet silicates. The terms enstatite bastite, tremolite bastite, talc bastite, etc. may be employed where distinction is possible. O'Hara (1967) has expanded the term bastite to include talc pseudomorphs after pyroxene, but this adds an unfortunate complication to the terminology and is not recommended.

Serpentinization of pyroxenes begins at grain boundaries and fractures, follows along cleavages and partings, and yields γ - or α -serpentine apparent fibers or laths lying parallel to the original cleavages. Orthopyroxenes tend to alter to γ -serpentine bastites (Fig. 2a) which usually appear to be fibrous, but may appear as nearly featureless plates (Fig. 2b). Variable amounts of α -serpentine may be present either randomly distributed, or as a marginal rim (Fig. 2c) or as a central core. A few orthopyroxene bastites are composed only of α -serpentine. In rare cases bastites may occur as a type of mesh texture (Fig. 2d and Rost 1959; Klinkhammer 1962; Peters 1963; Hochstetter 1965) or may be composed mainly of isotropic serpentine (Fig. 3a). Clinopyroxene exsolution lamellae, where serpentinized within orthopyroxene bastite, are no longer recognizable.

Clinopyroxene is serpentinized less easily than orthopyroxene, but can yield γ -serpentine bastites indistinguishable from orthopyroxene bastites (Leech 1953). However, some clinopyroxene

bastites observed in the present study (Fig. 3b) have been replaced by long thin zones of γ -serpentine "apparent-fibers" along cleavage planes or orthopyroxene exsolution lamellae, and by either elongate α -serpentine lamellae or nearly isotropic serpentine in the zones between cleavage traces.

Pyroxene bastites from twenty specimens were examined with 82 X-ray microbeam exposures (Table 1). Twelve (and probably another six) of these were orthopyroxene bastites, and one (and probably a second) was a clinopyroxene bastite (all mainly Type 3, Table 1). In every case but one, lizardite was the only serpentine mineral present, regardless of the optical characteristics of the serpentine or the type of bastite. In the exceptional case (18500, Type 5) the lizardite 1T of the bastite has minor amounts of chrysotile $2M_{cl}$ intimately associated with it, and in parallel growth with chrysotile $2M_{cl}$ in adjacent asbestos veins. In the lizardite described as α -serpentine, z is approximately parallel to α (similar to Fig. 6g in Wicks & Zussman 1975), in that described as γ -serpentine x is approximately parallel to γ (Figs. 6i, m in Wicks & Zussman 1975), and in that which is isotropic the lizardite is randomly oriented (similar to Fig. 6j in Wicks & Zussman 1975). The lizardite in all cases is the 1T polytype; however, some orthopyroxene bastites (18524, 18528, Type 3) also contain minor amounts of a 2-layer polytype.

Patches of parallel antigorite (γ -serpentine) lamellae resembling bastites (Hochstetter 1965; Boudier 1971) occur associated with some of the well-developed antigorite interpenetrating textures examined in this study (Fig. 3c). Hochstetter and Boudier identify these as antigorite bastites. No positively identified antigorite pseudomorphs after pyroxene were found in our study. All the pyroxenes, amphiboles or lizardite bastites partly replaced by antigorite were found to contain random antigorite blades developing towards interpenetrating textures, and so are not strictly pseudomorphic (Fig. 3d).

Accessory minerals are not commonly associated with bastites. Brucite occurs in intimate association with lizardite in bastites in only three samples (18529, 18552, 18554, Type 3, Table 1). In each case the presence of brucite is indicated by a yellowish to reddish brown color in plain light and an anomalous reddish birefringence under crossed nicols. These lizardite+brucite bastites are associated with lizardite+brucite mesh textures. Magnetite is generally not associated with pyroxene bastites. Only one specimen (18556, Type 3) has significant amounts of magnetite associated with the bastites. Seven others had traces of magnetite.

Amphiboles

Serpentinization of orthorhombic amphiboles (Winchell & Winchell 1959) or clin amphiboles

(Klinkhammer 1962; Hochstetter 1965) begins at grain boundaries, fractures, and cleavages, and can produce pseudomorphs resembling those after pyroxene. The serpentine formed

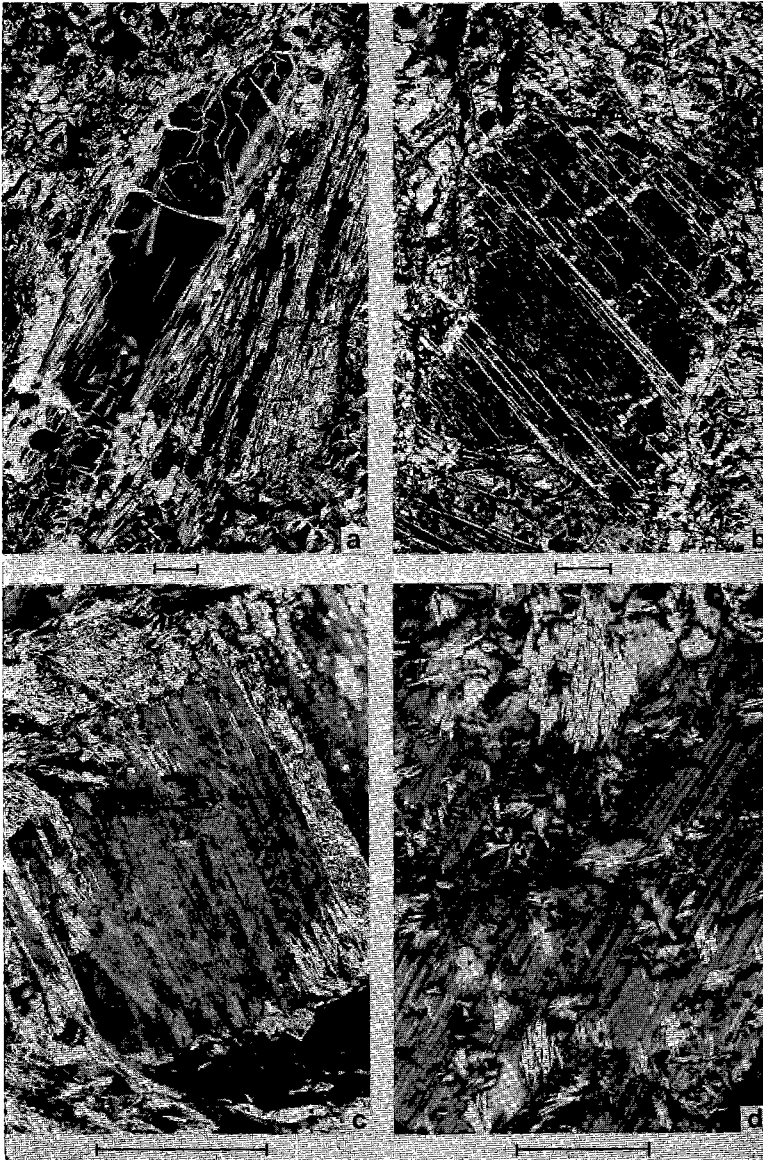


FIG. 3. (a) Lizardite 1*T* (mainly isotropic) bastite after orthopyroxene. Sample 18519, Glen Urquhart, Scotland. (b) Lizardite 1*T* bastite after clinopyroxene; γ -serpentine apparent fibers lie along cleavages with isotropic serpentine between them. Sample 18511, Lizard, England. (c) Possible antigorite bastite of uncertain origin. Sample 18524, Kaponigbach, Austria. (d) Randomly oriented antigorite blades which have replaced lizardite 1*T* (γ -serpentine apparent fibers) bastite after orthopyroxene. Sample 18556, Shulap Range, B.C. All under crossed nicols. Bar represents 0.2 mm.

along cleavages has no central parting although the serpentine formed along fractures does. Views down the z axis of the amphibole may show characteristic development of serpentine

zones along the cleavages (Fig. 4a). Views along other directions may show a set of cleavages filled with serpentine without a central parting and this set may be at right angles to a series

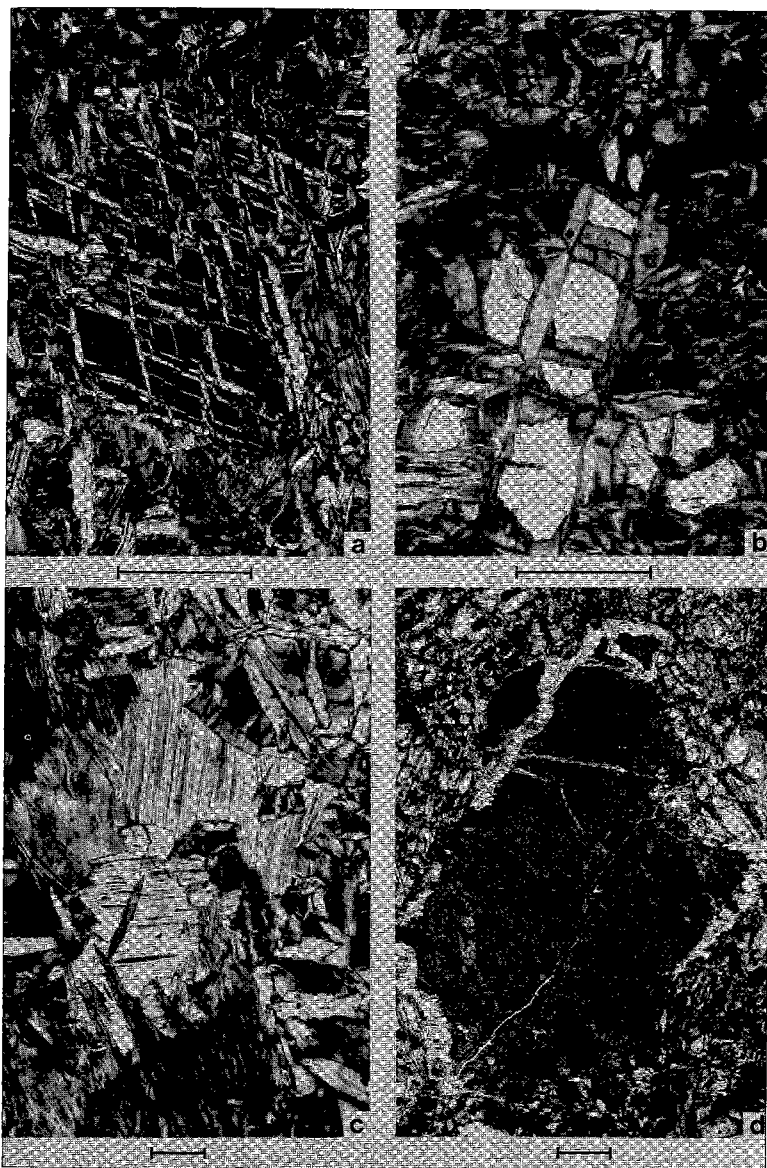


FIG. 4. (a) Lizardite 1T (γ -serpentine lamellae) which has replaced clinoamphibole along cleavage planes. Sample W68-6b, Brionde, France. (b) Lizardite 1T bastite after amphibole. The bipartite α -serpentine veins along the cross-cutting fractures, combined with the γ -serpentine along the cleavage, produce a mesh texture that strongly resembles mesh texture after olivine. Sample 18509, Glen Urquhart, Scotland. (c) Lizardite 1T and brucite (γ -serpentine apparent fibers) bastite after talc. Sample 18508, Glen Urquhart, Scotland. (d) Talc reaction rim on unserpentinized enstatite. Sample IB67-213, Bobtail Mountain, B.C. All under crossed nicols. Bar represents 0.2 mm.

of fractures filled with serpentine with a central parting. These two serpentine zones combine to produce mesh textures similar to those after olivine (Fig. 4b). However, mesh textures after

amphibole can be distinguished from mesh textures after olivine by the lack of a central parting in one set of mesh rims. The difference between such amphibole mesh textures and olivine

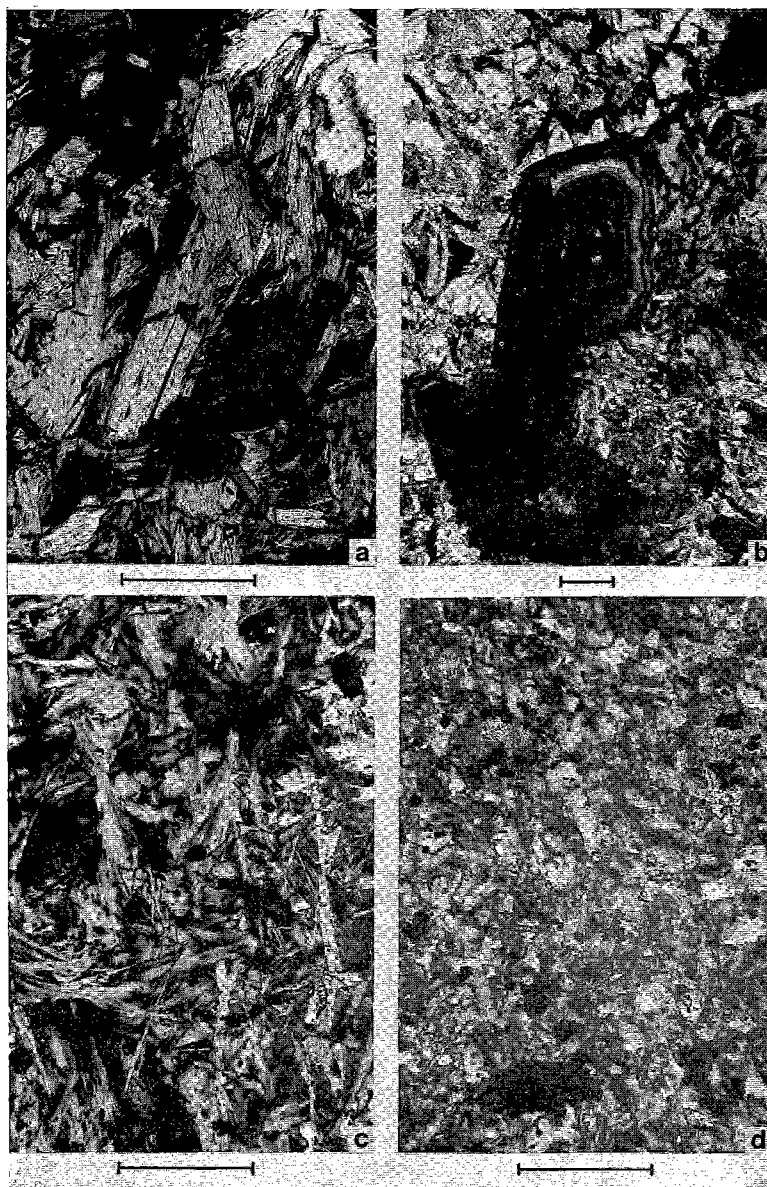


FIG. 5. (a) Antigorite (medium grey) which has partly replaced chlorite (pale grey) to produce bastite after chlorite. Sample 18518, Glen Urquhart, Scotland. (b) Lizardite 1T, both banded and featureless areas, after plagioclase. Sample 18478, Stillwater, Montana. (c) Antigorite interpenetrating texture. Sample 18523, Tasiussarssuaq Fjord, Greenland. (d) Antigorite and brucite interlocking texture. Anhedra brucite grains occur associated with anhedra magnetite grains in the middle of the NW quadrant and the east edge of the NE quadrant. Sample 18544, Jeffrey mine, Quebec. All under crossed nicols. Bar represents 0.2 mm.

mesh textures may have been overlooked previously (Fig. 4b). Weigand (1875) used the term window serpentine and trellis serpentine to describe these bastites, but Klinkhammer (1962) recommended that this use be discontinued.

Amphibole bastites from three specimens were examined with nine X-ray microbeam exposures (18509, 18550, 18562, Type 3, Table 1). α -serpentine, γ -serpentine and isotropic serpentine were examined. The serpentine in each was lizardite 1T, with z always approximately parallel to α and the isotropic material always having a random orientation. No brucite or magnetite was found associated with the amphibole bastites studied, although brucite occurs in the mesh textures after olivine in samples 18550 and 18562.

Talc, phlogopite and chlorite

Talc, phlogopite and chlorite can be replaced by γ -serpentine apparent fibers which develop along the original cleavages. Totally serpentinized talc forms bastites similar to orthopyroxene bastites (Fig. 4c). Frequently, the serpentinized talc rims around orthopyroxene are unrecognized and considered to be serpentine after orthopyroxene (Fig. 4d). This confusion further emphasizes why bastite should be used as a textural rather than a mineralogical term. Chlorite and phlogopite seem to be slightly less susceptible to serpentinization than talc, but they too can be altered (Fig. 5a). The pseudomorphic replacement of chlorite by a blade of antigorite (γ -serpentine) during the development of non-pseudomorphic textures has been described by Rost (1961), Klinkhammer (1962) and Klinkhammer & Rost (1967) (see section on Intermediate Textures).

Bastites of talc, phlogopite and, chlorite were examined from four specimens (18510, 18490, 18505, 18508, Type 3, Table 1) with 4 microbeam exposures. The phlogopite and chlorite bastites consist of lizardite 1T and the talc bastite is an intimate mixture of lizardite 1T and lesser brucite. All have the z axis approximately parallel to α . One chlorite bastite (18498, Type 7) was examined with three microbeam exposures and was found to be composed of antigorite with the y axis approximately parallel to γ (similar to Fig. 6o in Wicks & Zussman 1975).

Feldspar

Plagioclase is often replaced by chlorite prior to serpentinization (O'Hara 1967), and may be replaced by hydrogrossular (Smith 1958), thomsonite (Page 1976) or serpentine (Fig. 5b) during serpentinization. Serpentine after plagioclase often has a very fine-grained interlocking tex-

ture, or may be featureless, or may be marked by very fine concentric banding. α -serpentine, γ -serpentine or isotropic serpentine may be present as a very crude pseudomorph, recognizable mainly by the outline of the former plagioclase grain, which becomes much less distinct if pervasively serpentinized. The one specimen X-rayed with the microbeam camera was found to be lizardite 1T (18478, Type 3, Table 1).

NON-PSEUDOMORPHIC TEXTURES

Non-pseudomorphic textures are xenoblastic and form either through the recrystallization of pseudomorphic serpentine textures or, less frequently, directly through the serpentinization of primary olivine, pyroxene, amphibole etc. Non-pseudomorphic textures can be divided into interpenetrating (Fig. 5c) and interlocking (Fig. 5d) types. The serpentine grains in both are anhedral and mutually interfere, but tend to be elongate in interpenetrating textures and equant in interlocking textures. The orientation of the elongate grains may vary from completely random, in which case a massive rock is produced, to strongly subparallel orientation, in which case a foliated rock is produced. These textures have been described extensively (Angel 1930, 1964; du Rietz 1935; Selfridge 1936; Francis 1956; Gees 1956; Rost 1959; Green 1961; Chidester 1962; Klinkhammer 1962; Hochstetter 1965; Tröger 1969) although without X-ray identification the precise mineralogy of some of these textures remains in doubt.

In contrast to pseudomorphic textures, brucite in non-pseudomorphic textures is easily recognized as discrete anhedral grains (Figs. 5d, 8d) with creamy or anomalous brown or blue birefringence. Magnetite also occurs in discrete grains or lenses distributed throughout the textures. The color of the non-pseudomorphic serpentine usually varies with the grain size and distribution of the magnetite, becoming darker as the grain size decreases and as the grains are more uniformly dispersed.

Interpenetrating textures

Interpenetrating textures are composed of elongate blades, flakes, or plates that form a tight interpenetrating fabric (Fig. 5c). Francis (1956) used the term flame texture, and Green (1961) used the term thorn texture, to describe those consisting of antigorite.

Interpenetrating textures usually begin to develop as isolated flakes or blades, or fan-shaped bundles of blades (Angel 1930; Klinkhammer 1962) distributed throughout lizardite pseudomorphic textures (Fig. 3d) or primary silicates.

As recrystallization progresses, more and more blades form until they begin to interfere with one another, and develop an interpenetrating texture. Lizardite 1T mesh centers are a common, although not the only, place for this recrystallization to begin.

Eight γ -serpentine interpenetrating textures were examined with eleven microbeam X-ray exposures supplemented by two powder photographs (Table 2). Five of the eight γ -serpentine interpenetrating textures are composed of antigorite (Type 7, Table 2) in characteristic "flame" or "thorn" textures, with γ approximately parallel to γ (Figs. 6o,p in Wicks & Zussman 1975). The other three consist of chrysotile $2M_{c1}$ with visible brucite (18488, 18541, 18548, Type 5).

TABLE 2. X-RAY RESULTS ON NON-PSEUDOMORPHIC TEXTURES FROM VARIOUS ULTRAMAFIC BODIES

Location	Sample No.	Texture
<u>TYPE 5 SERPENTINIZATION</u>		
CHRYSOPILE + BRUCITE \pm MAGNETITE		
<i>concentrically zoned intrusions</i>		
Tulameen, B.C.	18488	γ -inpen, γ -ser vn
<i>alpine-type intrusions</i>		
Jeffrey mine, Quebec	18541	γ -inpen, γ -ser vn
	18548	γ -inpen, γ -ser vn
CHRYSOPILE + LIZARDITE 1T \pm MAGNETITE		
<i>alpine-type intrusions</i>		
Jeffrey mine, Quebec	18543	γ -inlock
CHRYSOPILE + LIZARDITE 1T + BRUCITE \pm MAGNETITE		
<i>alpine-type intrusions</i>		
Cassiar mine, B.C.	18555	α -inlock
<i>Proterozoic low-grade metamorphic terrain</i>		
Porcupine mine, Ontario	18559	α -inlock
LIZARDITE 1T \pm MAGNETITE		
<i>Proterozoic high-grade metamorphic terrain</i>		
Setting Lake, Manitoba	18503	α -inlock
LIZARDITE (MULTILAYER) \pm MAGNETITE		
<i>stratiform intrusions</i>		
Stillwater, Montana	18479	α -inlock
<i>alpine-type intrusions</i>		
Mayaguez, Puerto Rico	18530	α -inlock spher
Mount Albert, Quebec	18550	α -inlock
<u>TYPE 7 SERPENTINIZATION</u>		
ANTIGORITE \pm MAGNETITE		
<i>stratiform intrusions</i>		
Stillwater, Montana	18481	γ -inpen
<i>alpine-type intrusions</i>		
Kapongibach, Austria	18524	γ -inpen *
Shulap Range, B.C.	18556	γ -inpen
<i>Proterozoic high-grade metamorphic terrain</i>		
Oswagan Lake, Manitoba	18498	γ -inpen
Tasussarsuaq Fjord, Greenland	18523	γ -inpen
ANTIGORITE + BRUCITE \pm MAGNETITE		
<i>alpine-type intrusions</i>		
Jeffrey mine, Quebec	18544	γ -inlock, γ -ser vn

18000 series = Oxford University accession numbers

α = α -serpentine; γ = γ -serpentine; inpen = interpenetrating; inlock = interlocking; ser vn = serrate vein; spher = spherulitic; B.C. = British Columbia.

*an interpenetrating texture with talc

The microbeam diffraction patterns of the chrysotile indicate that x is approximately parallel to γ (Figs. 6a,b,c in Wicks & Zussman 1975). The chrysotile may occur as recognizable fiber bundles, but its fibrous nature may not be visible in thin section, in which case it may closely resemble antigorite blades.

Interlocking textures

Interlocking textures are composed of irregular, equant (Fig. 5d), sometimes spherulitic grains (Fig. 6a) of serpentine that form a tight interlocking fabric. They develop as small isolated patches which grow and join together as recrystallization proceeds. Both α -serpentine and γ -serpentine have been identified where it has been possible to determine an elongation. Some of these textures have been described as rosette-serpentine (Peters 1963) and as radial fiber bundle serpentine (Lapham 1964).

Two γ -serpentine and six α -serpentine interlocking textures were examined with nine microbeam exposures and three powder photographs (Table 2). One of the two γ -serpentine textures is composed of antigorite with visible brucite (18544, Type 7, Table 2), with the γ of antigorite approximately parallel to γ . The second is composed of an intimate submicroscopic mixture of chrysotile $2M_{c1}$ and lizardite 1T (18543, Type 5). γ lies approximately parallel to x of the chrysotile and elements of x and y of the lizardite.

Three of the six α -serpentine interlocking textures (18479, 18530, 18550, Type 5) are composed of a multi-layer polytype of lizardite (Fig. 6n in Wicks & Zussman 1975), one (18503, Type 5) of lizardite 1T and the remaining two (18555, 18559, Type 5) of an intimate submicroscopic mixture of lizardite 1T and chrysotile $2M_{c1}$ with visible brucite.

SERPENTINE VEINS

Late veins of serpentine along fractures, shears and joint planes can be found to a greater or lesser degree in almost every serpentinite. The fractures may pinch, swell, and branch, and those that have been sheared have often been subjected to slippage in several successive directions and have highly polished slickensides. This highly sheared serpentine is the "fish scale" or "fish meat" serpentine of Cooke (1937) and the "Schalenserpentin" of Rost (1949, 1959), Klinkhammer (1962), and Hochstetter (1965). Slip-veins are not as frequently observed in thin sections as they are in hand specimens or in the field, because the slip-veins often occur in highly sheared and broken rock unsuitable for thin

sectioning, or because they occur along joint planes or shear surfaces that form the edges of

hand specimens, where they are less frequently preserved during sectioning. Vein serpentine is

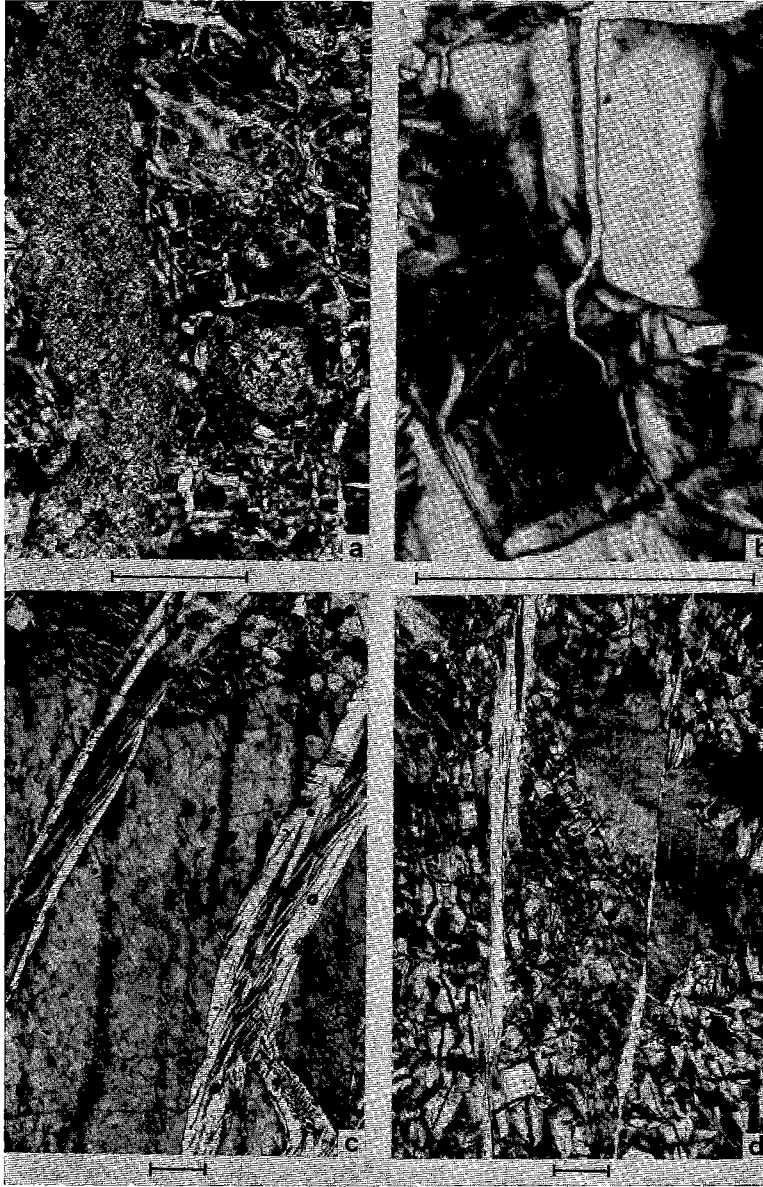


FIG. 6. (a) Multi-layer lizardite, fracture-filling vein of spherulitic and interlocking, radial apparent fiber bundles of α -serpentine. Similar textures have formed in the wall rock through recrystallization of the lizardite 1T mesh texture. Sample 18530, Mayaguez, Puerto Rico. (b) Chrysotile asbestos cross-fiber vein following a mesh rim parting (upper half) and then passing through a mesh center (lower half). Sample 18520, Glen Urquhart, Scotland. (c) Chrysotile asbestos cross-fiber vein with complex extinction patterns, cutting through a lizardite 1T bastite. Sample AG67-3c, Jeffrey mine, Quebec. (d) Chrysotile asbestos slip-fiber vein with associated parallel, thin, brucite fibers and magnetite pencils. Sample AG67-7a, Jeffrey mine, Quebec. All under crossed nicols. Bar represents 0.2 mm.

TABLE 3. X-RAY RESULTS ON SERPENTINE VEINS FROM VARIOUS ULTRAMAFIC BODIES

Location	Sample No.	Optical Character	Location	Sample No.	Optical Character
<u>TYPE 3 SERPENTINIZATION</u>			<u>TYPES 5 AND 7 SERPENTINIZATION</u>		
<u>ASBESTOS CROSS-FIBER VEINS</u> CHRYOSOTILE ± BRUCITE ± MAGNETITE			<u>ASBESTOS CROSS-FIBER VEINS</u> CHRYOSOTILE ± BRUCITE ± MAGNETITE		
<i>alpine-type intrusions</i>			<i>alpine-type intrusions</i>		
Mayaguez, Puerto Rico	18529	γ-fiber	Jeffrey mine, Quebec	18532	γ-fiber
<i>Precambrian high-grade metamorphic terrain</i>				18539	γ-fiber
Setting Lake, Manitoba	18503	γ-fiber		18540	γ-fiber
				18541	γ-fiber
				18545	γ-fiber
				18546	γ-fiber
<u>NON-ASBESTIFORM VEINS--FRACTURE FILLING</u> CHRYOSOTILE ± BRUCITE ± MAGNETITE			<i>Precambrian high-grade metamorphic terrain</i>		
<i>alpine-type intrusions</i>			Pipe Lake mine, Manitoba		
Mayaguez, Puerto Rico	18528	γ-app fiber		18499	γ-fiber
	18529	---		18500	γ-fiber
<u>LIZARDITE 1T ± BRUCITE ± MAGNETITE</u>			<u>NON-ASBESTIFORM VEINS--FRACTURE FILLING</u> CHRYOSOTILE ± BRUCITE ± MAGNETITE		
<i>alpine-type intrusions</i>			<i>alpine-type intrusions</i>		
Lizard, England	18511	α-app fiber	Jeffrey mine, Quebec	18546	---
	18513	near is			
Pinchi Lake, B.C.	18554	γ-app fiber	<u>CHRYOSOTILE + LIZARDITE 1T ± BRUCITE ± MAGNETITE</u>		
<i>Precambrian high-grade metamorphic terrain</i>			<i>alpine-type intrusions</i>		
Bucko Lake, Manitoba	18492	crystals	Jeffrey mine, Quebec	18547	---
Setting Lake, Manitoba	18504	---			
<u>CHRYOSOTILE + LIZARDITE 1T ± BRUCITE ± MAGNETITE</u>			<u>TYPE 6 SERPENTINIZATION</u>		
<i>stratiform intrusions</i>			<u>ASBESTOS CROSS-FIBER VEINS</u> CHRYOSOTILE ± BRUCITE ± MAGNETITE		
Fox River, Manitoba	18486	---	<i>alpine-type intrusions</i>		
<i>alpine-type intrusions</i>			Jeffrey mine, Quebec		
Lizard, England	18515	γ-app fiber*		18537	γ-fiber
Totalp, Davos, Switzerland	18527	γ-app fiber	<u>ASBESTOS SLIP-FIBER VEINS</u> CHRYOSOTILE ± BRUCITE ± MAGNETITE		
Mount Albert, Quebec	18549	near is*	<i>alpine-type intrusions</i>		
<i>Precambrian high-grade metamorphic terrain</i>			Jeffrey mine, Quebec		
Setting Lake, Manitoba	18507	---		18534	γ-fiber
				18536	γ-fiber
<u>TYPE 4 SERPENTINIZATION</u>			<u>NON-ASBESTIFORM VEINS--SLIP</u> CHRYOSOTILE ± BRUCITE ± MAGNETITE		
<u>NON-ASBESTIFORM VEINS--SLIP</u> LIZARDITE 1T ± BRUCITE ± MAGNETITE			<i>alpine-type intrusions</i>		
<i>alpine-type intrusions</i>			Jeffrey mine, Quebec		
Lizard, England	18515	γ-app fiber		18533	---
				18535	γ-fiber ^P
				18536	γ-fiber ^P
				18537	---
<u>TYPE 5 SERPENTINIZATION</u>			<u>CHRYOSOTILE + LIZARDITE 1T ± BRUCITE ± MAGNETITE</u>		
<u>NON-ASBESTIFORM VEINS--FRACTURE FILLING</u> LIZARDITE 1T ± BRUCITE ± MAGNETITE			<i>alpine-type intrusions</i>		
<i>Precambrian high-grade metamorphic terrain</i>			Jeffrey mine, Quebec		
Setting Lake, Manitoba	18503	α-inlock		18535	γ-fiber ^P
<u>LIZARDITE (MULTILAYER) + CHRYOSOTILE ± BRUCITE ± MAGNETITE</u>			<u>TYPE 7 SERPENTINIZATION</u>		
<i>stratiform intrusions</i>			<u>NON-ASBESTIFORM VEINS--FRACTURE FILLING</u> ANTIGORITE ± BRUCITE ± MAGNETITE		
Stillwater, Montana	18479	α** + γ-app fiber	<i>alpine-type intrusions</i>		
<u>LIZARDITE (MULTILAYER) ± BRUCITE ± MAGNETITE</u>			Mount Adstock, Quebec		
<i>alpine-type intrusions</i>				W70-45	γ-blades
Mayaguez, Puerto Rico	18531	α-spher inlock	<u>TYPE 8 SERPENTINIZATION</u>		
Pinchi Lake, B.C.	18554	α-spher inlock*	<u>NON-ASBESTIFORM VEINS--SLIP</u> ANTIGORITE ± BRUCITE ± MAGNETITE		
			<i>alpine-type intrusions</i>		
			Valtournanche, Italy		
				18526	γ-app fiber

18000 series = Oxford University accession numbers, W70 series = Wicks field number.

α = α-serpentine; γ = γ-serpentine; app = apparent; is = isotropic; inlock = interlocking texture; spher = spherulitic texture; B.C. = British Columbia.

Samples with no optical description were studied by 114.6 mm powder diffraction cameras and were not observed optically.

^PPovlen-type chrysotile

*with minor brucite

**lizardite 1T with minor multilayer lizardite

For simplicity, brucite is included as a possible accessory in all headings in this table. When it was recorded on a diffraction pattern, the entry is suitably marked. However, several veins also contain clearly distinguishable brucite, in hand specimen, which has not been noted in the table.

often distinctly green because any associated magnetite is usually segregated into coarse discrete grains. Good descriptive papers of vein morphology are those by Cooke (1937), Riordon (1955), and Merenko (1958).

Chrysotile asbestos cross-fiber veins

In fractures that have not been subjected to shear and in which chrysotile asbestos has developed, the chrysotile always appears as γ -serpentine in thin section. The finer veins may follow lines of weakness, such as the parting in a lizardite 1T mesh rim (Fig. 6b) or may cross-cut textural features (Fig. 6c). The fibers in small veins tend to lie normal to the walls and extend from one wall to the other without a break (Fig. 6b); larger veins commonly have a more or less central parting, often containing magnetite. Chrysotile fibers are usually visible in thin section and have parallel extinction, but some complex extinction patterns develop in cross-fiber veins which have kinks (Riordon 1955) through the combination of changing fiber direction and the oblique cut of the thin section (Fig. 6c). Fibers with anomalously high birefringence have been discussed by Wicks & Zussman (1975).

Eleven specimens were studied, six by microbeam camera, four by fiber camera, and one by powder photography (Type 3, Types 5 and 7, Type 6, Table 3). In all veins chrysotile $2M_{e1}$ is the main component, but some samples (18529, Type 3, 18541, Types 5 and 7, 18537, Type 6) contain minor, and in one case (18546, Types 5 and 7) major chrysotile $2Or_{e1}$. Others (18532, 18539, 18541, Types 5 and 7) contain minor parachrysotile. One sample (18541, Types 5 and 7) contains minor amounts of both parachrysotile and chrysotile $2Or_{e1}$. Brucite occurs as discrete grains or fibers in some specimens.

Chrysotile asbestos slip-fiber veins

Slip-fiber veins of asbestos can be seen, in thin section, to be composed of parallel to sub-parallel fibers of γ -serpentine lying parallel to, or at a low angle to, the enclosing vein walls (Fig. 6d). The fibers are generally visible, and the extinction varies from simple parallel to complex irregular patterns.

Two samples were X-rayed, one by fiber and one by powder techniques (18534, 18536, Type 6, Table 3). Chrysotile $2M_{e1}$ was identified as the main phase in both. Parachrysotile is present in minor amounts in one specimen (18534, Type 6) and traces of lizardite 1T were detected in the other (18536, Type 6). Brucite may be present as discrete fibers (Fig. 6d) or grains.

Non-asbestiform veins

These veins have different appearances in hand specimens and may be pseudofibrous, splintery, columnar, banded or massive. They are most frequently green with resinous luster, but may be dull or earthy and vary from white to black. The veins may occur in fractures that have experienced no movement, or in those that have experienced considerable shearing.

In thin section under crossed nicols, a great variety of textures is observed. The serpentine may appear to be columnar or pseudofibrous (Fig. 7a), banded parallel to the contacts (Fig. 7b), spherulitic (Fig. 7c), interlocking or interpenetrating grains or blades (Fig. 7d), or totally featureless. The extinction may be undulating or sweeping, or the serpentine may be isotropic. Where grains, blades or pseudofibers are visible, the fast- and slow-rays can be determined and the serpentine can be described as α - or γ -serpentine. In featureless serpentine the extinction positions are commonly approximately parallel and perpendicular to the vein walls so that fast- and slow-ray directions can be determined with respect to the vein walls. A great variety of combinations of textural features has been observed, with the serpentine in the wider (>0.15 mm) unsheared veins generally having a more complex textural development (Fig. 7c) and sometimes a central parting (Fig. 7a). Rarely, well-formed crystals of lizardite occur in veins (Fig. 8a). The slip-serpentine which formed in fractures which have undergone shearing is usually less complex. It resembles asbestos slip-fiber, in that it is often made up of γ -serpentine apparent fibers with the slow-ray subparallel to the shearing movement and the fiber axis, but is only pseudofibrous or splintery. In some cases composite veins have formed and several generations of serpentine, including asbestos, can be distinguished. Veins that have formed during shearing may pass into veins that have not undergone shearing. Serpentine may pass from non-fibrous to fibrous forms within a single vein.

Twenty-four specimens were studied, fourteen by microbeam camera, with 73 exposures, three by fiber photographs, and nine by powder photographs (Table 3). Lizardite 1T and chrysotile $2M_{e1}$ predominate, occurring both singly and together either as an intimate admixture or with segregation of one or other towards the vein walls. Five veins (18486, 18527, 18507, Type 3, 18546, Types 5 and 7, 18537, Type 6, Table 3) contain variable amounts of chrysotile $2Or_{e1}$, and two other veins (18535, 18536, Type 6) contain chrysotile which gives lines of the "Povlentype" (Krstanović & Pavlovic 1964; Middleton &

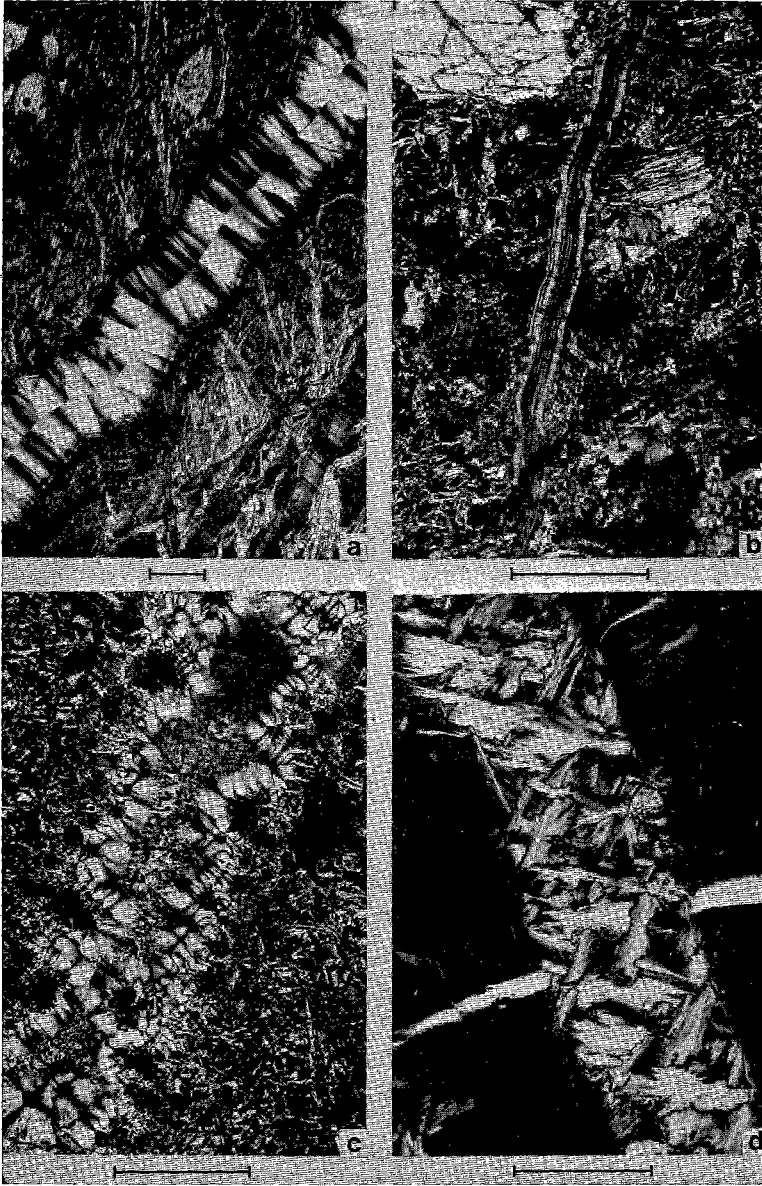


FIG. 7. (a) Vein composed of non-asbestiform chrysotile (γ -serpentine apparent fibers) in the columnar central zone, and lizardite 1T with minor multi-layer polytype (α -serpentine) in the banded, nearly isotropic, marginal zones. Sample 18479, Stillwater, Montana. (b) Vein composed of lizardite 1T (α -serpentine apparent fibers and isotropic serpentine) banded parallel to contacts. Sample 18513, Lizard, Cornwall. (c) Complex vein composed of lizardite 1T (α -serpentine apparent fibers) in radial bundles and some spherulites (SW corner), lizardite 1T \pm chrysotile $2M_{c1}$ \pm brucite in the marginal isotropic loops, and lizardite 1T and/or chrysotile $2M_{c1}$ in the fine-grained and isotropic central zone. Sample 18515, Lizard, Cornwall. (d) Fracture-filling vein composed of antigorite interpenetrating blades which partly replace the host lizardite 1T (NW corner). Sample W70-45 Mount Adstock, Quebec. All under crossed nicols. Bar represents 0.2 mm.

Whittaker 1976; Cressey & Zussman 1976). One in eleven lizardite $1T$ diffraction patterns also contains some lizardite $2H$. Multi-layer lizardite polytypes make up two veins (18531, 18554, Type 5) and occur in minor amounts in a third (18479, Type 5). Antigorite occurs in two veins (W70-45, Type 7, 18526, Type 8). The lizardite crystals (18492, Type 3) were identified as the $1T$ polytype. Brucite may occur either as discrete grains or in an intimate admixture with the serpentine minerals (18515, 18549, Type 3, 18554, Type 5). The only cases in which optical identification of the serpentine seems to be possible is the rare occurrence of antigorite (γ -serpentine) which can be recognized from its characteristic bladed morphology (Fig. 7d), and the more abundant, fibrous, bladed, or spherulitic α -serpentine which seems to be lizardite, usually a multi-layer polytype (Fig. 6a). The common γ -serpentine apparent fibers are usually chrysotile and/or lizardite. The only specific textural generalization is that the coarseness of crystallinity of lizardite, as indicated by spots on the microbeam diffraction patterns, increases toward the margins of veins, but exceptions were noted.

The non-asbestiform veins discussed in this section have been called picrolite by Riordon (1955), and this term is in current usage in the asbestos mining industry. However, the name picrolite was originally applied to a fibrous vein material by Hausmann (1808). This type material was shown by Whittaker & Zussman (1956) to be antigorite, and they recommended that the name, if retained, should be restricted to distinctly fibrous or splintery antigorite. Earlier workers on the asbestos deposits of the Eastern Townships, Quebec (Cooke 1937) seem to have applied the name to fibrous veins of non-chrysotile-like material, and this usage has gradually been extended to cover all non-asbestiform veins whether fibrous or not. The work described here shows that this extension of meaning makes picrolite into a purely textural field term devoid of mineralogical meaning. The term serpo-phite has been used by Lodochnikov (1933) and Merenkov (1958) to describe these vein serpentine, but we prefer to confine this term to isotropic serpentine in mesh centers.

INTERMEDIATE TEXTURES

The above classification of textures into pseudomorph, non-pseudomorph, and vein types is in some respects an idealization and the divisions, in some cases, are gradational.

Some antigorite and chrysotile pseudomorph

textures (Table 1) represent an early stage in the development of interpenetrating or interlocking textures of the same minerals (Table 2). In particular, relict olivine in lizardite mesh textures readily alters to crude antigorite or chrysotile pseudomorphs (Figs. 8b,c); however, their prominence decreases as their outlines become blurred by the extensive formation of interlocking and interpenetrating textures. Similarly, although the antigorite pseudomorphs after chlorite are a faithful replacement (Fig. 5a), once the chlorite alteration is complete the pseudomorphs become indistinguishable from the surrounding antigorite in the enclosing interpenetrating texture. Also, in some cases, chlorite is not replaced by antigorite in an orderly manner, but is replaced by random interpenetrating blades of antigorite. The antigorite bastites described by Hochstetter (1965) and Boudier (1971) also may fall into this group of textures.

Hairline fractures across pseudomorph or non-pseudomorph textures, or between serpentinized and relict olivine, are often the site of the beginning of recrystallization and lead to the development of vein-like textures (Fig. 8d). These often have serrate boundaries rather than the smooth walls of typical veins, and Riordon (1955) called them "serrated veins". They are, however, recrystallization features and not fracture-filling veins, although serrate veins of asbestos are closely associated with the formation of cross-fiber asbestos veins. In a rectilinear set of closely spaced fractures, the serrate veins can give rise to crude hourglass textures (Fig. 1d).

Four samples containing serrate veins were X-rayed with four microbeam exposures. Three (18488, 18541, 18548, Type 5, Table 2) were found to be composed of chrysotile $2M_{c1}$, two (18541, 18548, Type 5) with minor chrysotile $2O_{r_{c1}}$, and one (18544, Type 7) of antigorite. All are associated with discrete brucite grains (Fig. 8d).

Some non-asbestiform fracture-filling veins are associated with recrystallization of the wall-rock serpentine to non-pseudomorph textures similar to the textures in the veins (Figs. 6a, 7d). The parallel growth between chrysotile in asbestos veins and in adjacent bastites, described in the pyroxene section above, is a similar phenomenon.

Non-asbestiform slip veins are often intimately associated with, and in parallel orientation to, foliated non-pseudomorph textures in the host rock, so that the margin between vein and host rock is uncertain. Non-asbestiform veins also grade and merge into chrysotile asbestos veins, and more or less isolated pockets of each may be present in the other.

IDENTIFICATION CHART

The results of the X-ray study are summarized in Table 4 which can be used as an identification

chart for petrographic studies. In some cases predictions can be made from Table 4 with a high degree of certainty, but in others the certainty is not high. The data further emphasize

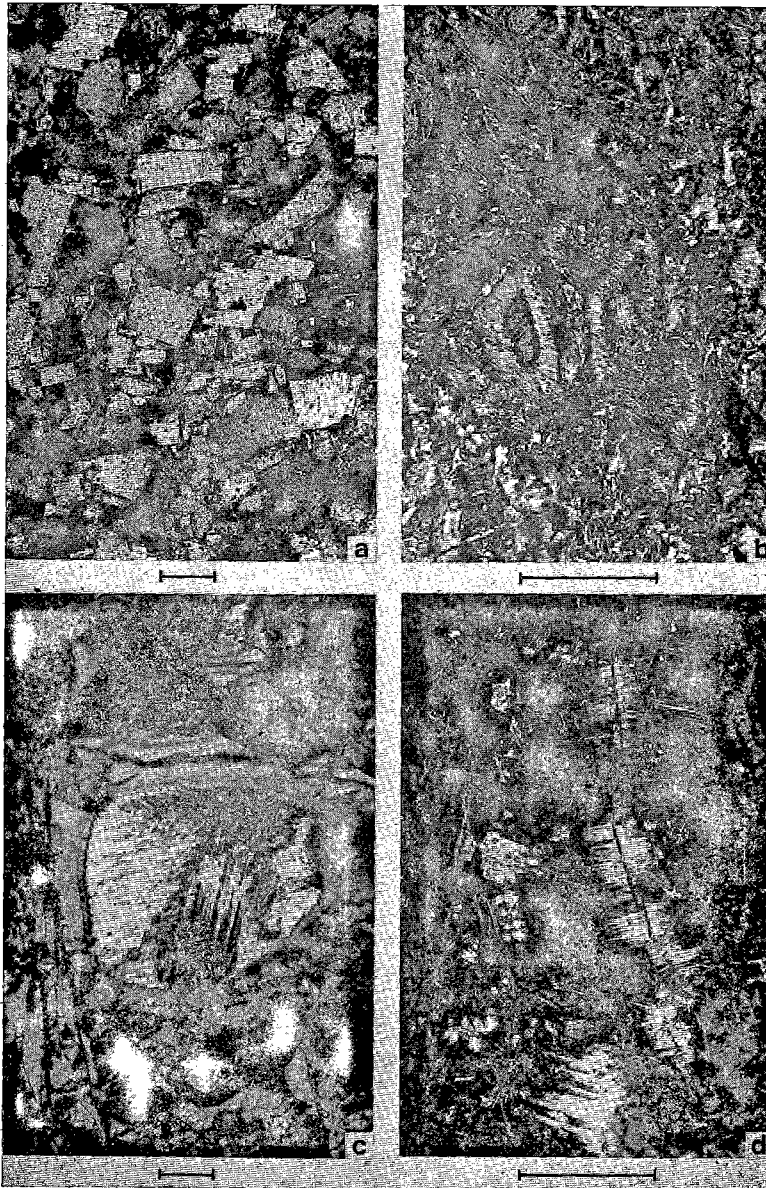


FIG. 8. (a) Lizardite 1T crystals in a fracture-filling vein. Sample 18492, Bucko Lake, Manitoba. (b) Antigorite which has replaced olivine to produce crude lens-shaped pseudomorphs. Sample 18481, Stillwater, Montana. (c) Chrysotile $2M_{c1}$ and $2O_{r1}$ mesh center, after olivine within lizardite 1T mesh rims. Sample 18538, Jeffrey mine, Quebec. (d) Chrysotile $2M_{c1}$ and minor $2O_{r1}$ serrate asbestos veins replaced non-fibrous chrysotile. Brucite is visible as discrete anhedral grains in the serrate veins and the groundmass. Sample 18548, Jeffrey mine, Quebec. All under crossed nicols. Bar represents 0.2 mm.

that the terms α - and γ -serpentine have no strict mineralogical meaning (Wicks & Zussman 1975).

Pseudomorphic textures usually consist of lizardite 1T, and are therefore a good determinant of this mineral. The only exceptions are antigorite or chrysotile pure hourglass textures and mesh centers, and antigorite bastites after chlorite. However, these textures only occur infrequently through the serpentinization of relict primary minerals, usually at the same time as lizardite 1T \pm brucite pseudomorphic textures are recrystallized to antigorite or chrysotile non-pseudomorphic textures. Therefore, they can often be identified by this association. The presence or absence of brucite in pseudomorphic textures can be determined only by X-ray diffraction.

Non-pseudomorphic textures consisting of α -serpentine can also confidently be expected to consist mainly of lizardite 1T, or multi-layer polytypes (though minor chrysotile, usually 2M_{cl}, may be present as well), but those consisting of γ -serpentine are variable. Antigorite is most common, and generally forms easily recognized interpenetrating textures composed of sharp distinct blades. Chrysotile, mainly 2M_{cl}, and/or lizardite 1T, often form interlocking textures composed of less distinct grains, but exceptions are common. The refractive indices of antigorite generally are higher than those of chrysotile or lizardite, but there is a considerable overlap among the ranges of the indices of all three minerals (Wicks & Zussman 1975). Extinction in antigorite blades usually sweeps across the blade, whereas in chrysotile fibers the extinction usually sweeps along the length of the fibers. However, not all chrysotile appears to be fibrous and often it is not possible to distinguish antigorite, chrysotile and/or lizardite without relying on X-ray diffraction. Brucite is easily identified in non-pseudomorphic textures because it is present as discrete grains.

Chrysotile asbestos, both in fracture-filling and slip veins, can be identified in thin section with great confidence. The α -serpentine interlocking spherulitic textures in veins are usually, but not always, multi-layer lizardite. Antigorite veins usually can be recognized by the characteristic appearance of the antigorite blades, but many non-asbestiform veins are composed of chrysotile or lizardite, or both, in intimate association. There is no optical criterion that can be used to differentiate these, and X-ray studies are essential for identification. Povlen-type chrysotile is not uncommon. In lizardite, 1T is the common polytype, but the 2H polytype occurs more frequently in veins than in pseudomorphic textures. Brucite may again occur in the veins

TABLE 4. SERPENTINE IDENTIFICATION CHART FOR THIN SECTIONS

Texture	Optical Character	Mineralogy
PSEUDOMORPHIC TEXTURES*		
mesh rim	α γ	lizardite** \pm brucite lizardite, antigorite or chrysotile
mesh center	α , γ + is	commonly lizardite \pm brucite, rarely antigorite or chrysotile \pm brucite
hourglass	α γ	lizardite \pm brucite antigorite or chrysotile
orthopyroxene-bastite	α γ	lizardite, rarely with brucite lizardite, rarely with brucite
clinopyroxene-bastite	α γ	lizardite lizardite
amphibole-bastite	α γ	lizardite, rarely with brucite lizardite, rarely with brucite
phlogopite-bastite	α γ	not found lizardite, rarely with brucite
talc-bastite	α γ	not found lizardite, rarely with brucite
chlorite-bastite	α γ	not found antigorite or lizardite
NON-PSEUDOMORPHIC TEXTURES*		
interlocking	α γ	lizardite 1T or multilayer polytype, possibly with some chrysotile chrysotile and/or lizardite or antigorite
interpenetrating	α γ	not found commonly antigorite, less commonly chrysotile and/or lizardite
serrate veins	α γ	not found commonly chrysotile, less commonly antigorite
VEIN SERPENTINE*		
asbestos cross-fiber	α γ	not found chrysotile
asbestos slip-fiber	α γ	not found chrysotile
non-asbestiform (fracture filling)	α γ is	lizardite 1T or multilayer polytypes chrysotile and/or lizardite or antigorite \pm brucite chrysotile and/or lizardite \pm brucite
non-asbestiform (slip)	α γ is	not found chrysotile and/or lizardite or antigorite \pm brucite chrysotile and/or lizardite \pm brucite

is = isotropic

*Brucite can very rarely be identified with the microscope in pseudomorphic textures and some non-asbestiform veins, so the possibility of its presence is included in these parts of the table. It can, however, usually be identified optically in non-pseudomorphic textures and fiber veins, so mention of it is omitted from these sections.

**Lizardite usually occurs as the 1T polytype, and occasionally there are minor amounts of a 2H polytype. The occurrence of other multilayer lizardite is specifically noted in the table.

either as an unrecognizable intimate mixture with chrysotile or lizardite, or as recognizable discrete grains.

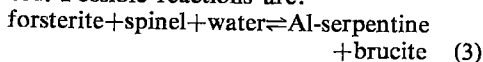
THE PROCESS OF SERPENTINIZATION

Review of phase studies

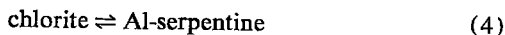
Any discussion of the implications of the foregoing sections for the process of formation of the serpentinites must be based on available knowledge of phase stabilities. The reaction

forsterite + water \rightleftharpoons serpentine + brucite (1) has been shown by Johannes (1968) to occur at 380°C at 2 kbars, and

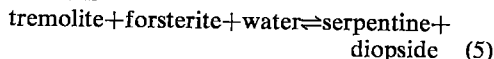
forsterite + talc + water \rightleftharpoons serpentinite (2) occurs at 460° (Scarfe & Wyllie 1967) or 440° (Chernosky 1971) at the same pressure. The effect of iron in the system is to slightly reduce these maximum temperatures (Olsen 1963; Moody 1976). There are indications from the work of Yoder (1952) and Chernosky (1971, 1975) that the upper stability limit of serpentinite is raised by the presence of Al, although it is not clear that all the reactions quoted have been reversed. Possible reactions are:



and



The serpentinization of diopside and tremolite involves the consideration that either silicon must be removed or an extraneous source of magnesium must be available, the effect being more marked in diopside. In either case calcium must be removed from both minerals. The process that is geologically most relevant is the addition of magnesium provided by forsterite as in the reaction



proposed by Evans & Trommsdorff (1970), which has an equilibrium temperature between those of (1) and (2).

Chrysotile has been synthesized in the pure MgO-SiO₂-H₂O system (Yoder 1952; Roy & Roy 1954; Gillery 1959; Johannes 1968) and co-existing chrysotile and lizardite 1T in the presence of small proportions of iron (Moody 1976) and alumina (Gillery 1959; Chernosky 1971, 1975). At higher alumina concentrations, lizardite 1T and (increasingly) multi-layer lizardite polytypes are produced. However, a 6-layer lizardite polytype also seems to have been produced in the alumina-free system by Jasmund & Sylla (1971, 1972). Antigorite has been synthesized (with coexisting chrysotile and lizardite) by Iishi & Saito (1973), but only when the ratio of MgO:SiO₂ was lower than 3:2. They found antigorite formation to be promoted by limited availability of water, and by higher temperatures and pressures. Other reported syntheses of antigorite are those by Korytkova & Makarova (1971), Korytkova *et al.* (1972), Johannes (1975) and Evans *et al.* (1976). General evidence that antigorite, although less readily synthesized, is more stable than the other serpentinite minerals comes from DTA evidence (Faust & Fahey 1962), structural considerations (Wicks & Whitaker 1975), field studies of metamorphosed serpentinites (Hess *et al.* 1952; Hahn-Weinheimer & Rost 1961; Chidester 1962; Wolfe 1967; Dietrich & Peters 1971; Keusen 1972;

Bucher & Pfeifer 1973; Trommsdorff & Evans 1972, 1974; Vance & Dungan 1977), and thermochemical calculations (King *et al.* 1967; Evans *et al.* 1976). This evidence suggests that the equilibrium temperatures of reactions 1 to 5 involving antigorite are higher than those involving lizardite or chrysotile.*

The above results can be unified schematically, as in the first two sections of Figure 9, to provide a basis for the interpretation of the textures identified in this paper. The discussion of the relationship between the temperature scales of the two and the effect of pressure are beyond the scope of this paper, but are discussed, at least for chrysotile and antigorite, by Evans *et al.* (1976). The evidence suggests that lizardite and chrysotile behave similarly (Dungan 1977). Since it seems clear that metastable relationships among the various serpentinite minerals are widespread, one may deduce in the simplest case the existence of not less than three temperature ranges corresponding to different assemblages as shown in the third section of Figure 9. The evidence presented in Figure 4 in Evans *et al.* (1976) suggests that the reactions F+Ta+W \rightleftharpoons (L+C) and F+W \rightleftharpoons A+B do not occur at the same temperatures as suggested in Figure 9, but for the purpose of our discussion this simplified form will be used.

General considerations of starting materials and temperature

Ultramafic rocks, whether dunite, harzburgite, lherzolite, wehrlite etc. and whether plagioclase-, spinel- or garnet-bearing, can be subjected to significant alteration prior to, and unrelated to, serpentinization. With cooling from high temperatures in the presence of water, rocks of these compositions can produce clino-amphiboles, chlorite, anthophyllite and talc successively (Fig. 1.4 in O'Hara 1967; Fig. 2 in Evans & Trommsdorff 1970). The complete cooling sequence of reactions has been observed in the Glen Urquhart ultramafic rocks (Francis 1956) included in the present study. Any or all of these minerals along with olivine, orthopyroxene and clinopyroxene may be present at the commencement of serpentinization and may themselves be serpentinized. Progressive metamorphism of a serpentinite will produce the same min-

*While our paper was in press our attention was drawn to two papers, both by Hemley *et al.* (1977), which have a bearing on the possible equilibrium relationships among antigorite, chrysotile, and brucite, and other equilibrium and non-equilibrium processes involved in serpentinization.

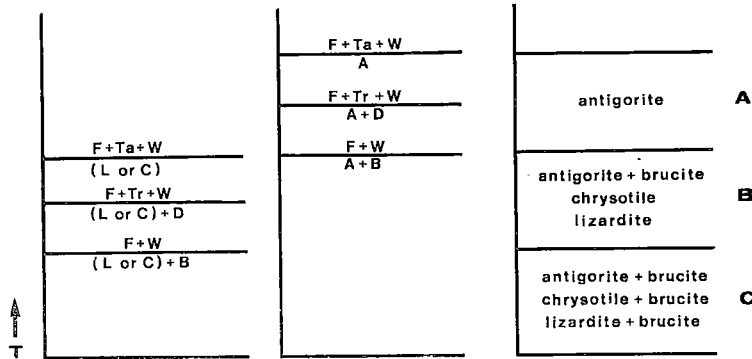


FIG. 9. Schematic diagram of the temperature regimes of the observed assemblages. Abbreviations for minerals in the equilibria: A=antigorite, B=brucite, C=chrysotile, D=diopside, F=forsterite, L=lizardite, Ta=talc, Tr=tremolite, W=water. The three temperature regimes are denoted A, B, C on the extreme right of the diagram.

eral assemblages (Evans & Trommsdorff 1970; Trommsdorff & Evans 1974; Evans *et al.* 1976) which in turn may be serpentinized at some later period.

It is important to note that the experimental studies described above, and summarized schematically in Figure 9, indicate only maximum temperatures of serpentinization. It is clear from recent isotropic studies (Wenner & Taylor 1971, 1973, 1974; O'Neill & Barnes 1971; Magaritz & Taylor 1974; Barnes & O'Neill 1969; Barnes *et al.* 1972) that much serpentinization occurs at temperatures well below these upper limits, and probably in regimes of substantially constant temperature. This is entirely consistent with Figure 9, requiring only that the rate-limiting factor in serpentinization be the availability of water rather than temperature.

A model of the serpentinization process

A possible model of the serpentinization process, which takes account of the available experimental evidence summarized in Figure 9, provides a framework into which the observations on the various textures may be fitted. The model provides eight distinguishable regimes in terms of all combinations of the following three alternatives.

- a. (i) falling (or constant) temperature
- (ii) rising temperature
- b. (i) absence of substantial shearing
- (ii) presence of substantial shearing
- c. (i) nucleation of antigorite
- (ii) no nucleation of antigorite

The physical or chemical conditions corresponding to (c) cannot at present be identified fully, but experimental work over the past 25 years

has strongly suggested that nucleation of antigorite is an improbable process in many circumstances. The absence of shearing, and falling or low constant temperature, may be expected to promote the formation of pseudomorphic textures, which may be disrupted by shearing to produce non-pseudomorphic textures and some veins. Under rising temperature conditions, recrystallization to form mainly non-pseudomorphic textures is promoted. The eight types are discussed in sequence beginning with high temperature, going down to low temperature and then back up to high temperature. Within each temperature regime the unsheared assemblage is discussed first followed by the sheared assemblage.

The eight types of process are therefore as follows:

1. a(i)+b(i)+c(i) Serpentinization begins at the highest possible temperature and gives rise to antigorite pseudomorphic textures in regime A in Figure 9. Fracture-filling veins produced with this type will be composed of antigorite.
2. a(i)+b(ii)+c(i) As type 1 but produces foliated non-pseudomorphic textures.
3. a(i)+b(i)+c(ii) Serpentinization is delayed to lower temperatures and gives rise to pseudomorphic textures of lizardite in regime B or lizardite±brucite in regime C. Chrysotile does not usually occur in abundance in the pseudomorphs, but may occur in veins along joint planes with or without lizardite and brucite.
4. a(i)+b(ii)+c(ii) As type 3 but produces foliated chrysotile±brucite non-pseudomorphic textures, with or without lizardite, and chrysotile±lizardite±brucite veins.

5. a(ii)+b(i)+c(ii) Rising temperature produces the recrystallization of lizardite±brucite pseudomorph textures of type 3, or the serpentinization of relict primary minerals to form non-pseudomorph textures of chrysotile±lizardite±brucite with associated veins of similar mineralogy in regimes B and C. Relict olivine may be serpentinized to crudely pseudomorph textures of chrysotile±brucite. (See below for the association of the chrysotile textures with asbestos vein development). Interlocking non-pseudomorph textures and associated veins of multi-layer lizardite without chrysotile are a minor variation of this type.
6. a(ii)+b(ii)+c(ii) As type 5 but produces either chrysotile±lizardite±brucite, or, less frequently multi-layer lizardite±brucite, foliated non-pseudomorph textures and veins.
7. a(ii)+b(i)+c(i) Continued rising temperature produces recrystallization of type 3 serpentine textures, or the serpentinization of previously un-serpentinized primary minerals and gives rise to non-pseudomorph textures, and occasionally crude pseudomorph textures of antigorite+brucite in regimes B and C, and of antigorite in regime A. (See below for the association of antigorite+brucite textures with asbestos vein development).
8. a(ii)+b(ii)+c(i) As type 7 but produces foliated non-pseudomorph textures of antigorite±brucite.

The problem of the relative volumes of the primary minerals and of the serpentinized products has to be considered at this point (for discussions on serpentinization at constant volume versus constant composition see Hostetler *et al.* 1966; Thayer 1966, 1967; Page 1967b, 1976*; Gresens 1967, 1969; Thompson 1968; Coleman 1971; Coleman & Keith 1971; Martin 1971; Clark & Greenwood 1972). This problem always affects processes 1 to 4 significantly and will affect similarly processes 5 to 8 if they operate on un-serpentinized peridotite. If processes 5 to 8 operate on previously formed serpentine, they are predominantly recrystallization processes and little volume or composition change will occur. We take the view that the pseudomorph textures produced by processes 1 and 3 require that serpentinization be a topotactic

process which, on a grain-for-grain basis, should involve but little volume increase. In some cases radial cracks which occur in plagioclase (Flett 1946; Smith 1958; Page 1976) and diopside (Clark & Greenwood 1972) adjacent to serpentinized olivines, undoubtedly represent some expansion. Observations of thin sections can reveal only linear expansions and these are one-third of volume expansion. Volume increases of between 25 and 45% have been calculated for complete serpentinization. These would produce linear expansions of 8 and 13%, respectively, and would cause much greater disruption of the enclosing minerals than is observed. The radial cracks, therefore, represent a much smaller volume increase. There will be, of course, an overall expansion in the body corresponding to the volume occupied by the ever-present serpentine veins, and to the volume occupied by some of the serpentine in the shear zones usually found adjacent to the contacts (processes 2 and 4). On the basis of the assumption of a topotactic process with little volume increase, one may treat the various serpentinization reactions on the basis of the preservation of the number of oxygen atoms in the (weighted mean) formula of the primary minerals. This means that the anion framework of close-packed oxygens remains almost unchanged by serpentinization and leads to the results given in Table 5.

It is evident from Table 5 that only forsterite and enstatite can alter to serpentine without the addition of magnesium from an outside source. Anthophyllite, talc, tremolite, and diopside all require an outside source of magnesium, and forsterite is the only possible magnesium source. Furthermore, only those reactions which produce excess of both Mg and Si can contribute to the formation elsewhere of vein-filling serpentine in fractures or shear zones. The most appropriate reactions in this respect are:

forsterite → lizardite + brucite
and

forsterite + (enstatite or anthophyllite) → lizardite
because of the ratio of Mg:Si in their excess products.

When one considers that some iron usually substitutes for magnesium in these minerals, it becomes clear why the production of secondary magnetite is almost always confined to the serpentinization of olivine, as it is the only mineral that liberates significant amounts of its cation content during serpentinization.

Interpretation of the observed textures

The observed textures may be classified in terms of the types of processes that would be expected to produce them according to our model.

*Page (personal communication). There are miscalculations on page 136 of Page (1976). For a volume increase of 37% the linear expansion should read 11% (not 3.3%), and for a volume increase of 19% the linear expansion should read 6% (not 2.7%).

TABLE 5. REQUIREMENTS AND REACTION PRODUCTS OF SERPENTINIZATION BASED ON 72 OXYGENS

Primary mineral	Product in situ	Reactant needed to complete constant volume reaction	Excess to be carried away or to provide reaction product elsewhere
forsterite	lizardite	32H ⁺	12Mg ²⁺ + 25Si ⁴⁺
forsterite	lizardite + brucite*	42H ⁺	9Mg ²⁺ + 6Si ⁴⁺
enstatite	lizardite	32H ⁺	8Si ⁴⁺
anthophyllite	lizardite	3Mg ²⁺ + 26H ⁺	8Si ⁴⁺
talc	lizardite	6Mg ²⁺ + 20H ⁺	8Si ⁴⁺
tremolite	lizardite	9Mg ²⁺ + 26H ⁺	8Si ⁴⁺ + 6Ca ²⁺
diopside	lizardite	12Mg ²⁺ + 32H ⁺	8Si ⁴⁺ + 12Ca ²⁺
<u>Primary assemblage on a 1:1 basis</u>			
forsterite + enstatite	lizardite	64H ⁺	12Mg ²⁺ + 10Si ⁴⁺
forsterite + anthophyllite	lizardite	58H ⁺	9Mg ²⁺ + 10Si ⁴⁺
forsterite + talc	lizardite	52H ⁺	6Mg ²⁺ + 10Si ⁴⁺
forsterite + tremolite	lizardite	58H ⁺	3Mg ²⁺ + 10Si ⁴⁺ + 6Ca ²⁺
forsterite + diopside	lizardite	64H ⁺	10Si ⁴⁺ + 12Ca ²⁺

*Based on 72 oxygens and a 3:1 ratio of serpentinite:brucite.

For heading "Reactant needed . . ." read Reactant needed to complete topotactic reaction.

Type 1. Only one example of this has been observed in the present work, namely the pseudomorphous antigorite after olivine of the Fox River Sill peridotites (Table 1). The veins associated with these textures are composed of antigorite. The antigorite textures in a similar environment described by Varlakov (1975) are non-pseudomorphous and therefore their relationship to this type seems doubtful.

The γ -serpentine mesh textures in the Telson Lake and Tadmagouche Creek sills (Table 1) could easily be mistaken, under the microscope, for further examples but the X-ray microbeam results demonstrate them to be lizardite in an unusual orientation.

Type 2. No example of this type was found in the present work, but possibly some of the foliated antigorite in the Iherzolite of the Lanzo Massif (Nicolas 1967, 1969) represents this type.

Type 3. This type appears to be the most common, as is indicated by the majority of our specimens (Table 1). The serpentization of olivine by this process leads to the formation of mesh rims by a steadily advancing front of serpentization that produces reasonably well-crystallized and crudely oriented lizardite (Wicks & Zussman 1975; Wicks *et al.* 1977). In some cases the front advances uniformly without a break until all the olivine is replaced and lizardite 1T±brucite pure hourglass textures are formed. Pure hourglass textures occur most frequently in association with Type 5 textures, suggesting that the formation of both is promoted by higher temperatures.

More often, the front stops at some point either because of cooling or lack of water, or possibly because the reaction changes from being interface-controlled to being diffusion-controlled (Martin & Fyfe 1970). The remnant olivine fragments may subsequently serpentize to produce mesh centers of poorly crystalline, fine-grained, semi-randomly to randomly oriented grains of lizardite 1T (Wicks & Zussman 1975) with possibly minor chrysotile (Cressey & Zussman 1976). This mesh-center serpentization takes place simultaneously throughout the olivine remnant, in contrast to the advancing front of serpentization that produces the mesh rims and pure hourglass textures. The lizardite produced often has some orientation in sympathy with the adjacent, earlier-formed mesh rim, although it seems more randomly oriented, a change that is difficult to explain. Where brucite is present, there is a strong tendency for it to occur, with lizardite, in the mesh centers surrounded by lizardite mesh rims. However, the reverse situation with lizardite+brucite mesh rims and lizardite mesh centers has also been recorded (Glen Urquhart and Mount Albert, Table 1). These differences in brucite distribution could be associated with temperature regimes B and C of Figure 9, but they are more likely to be due to varying kinetic effects on the amount of magnesium removed in solution. Orthopyroxenes also alter to lizardite pseudomorphs. These generally are free of brucite and magnetite in accordance with the fact that no octahedral cations need be lost (or gained) in a topotactic serpentization of orthopyroxene, but rarely some

lizardite bastites contain brucite near the center of the pseudomorph (Mayaguez, Mount Albert, Pinchi Lake, Table 1). This requires a complete loss of silicon and an addition of $\frac{1}{3}$ again the number of octahedral cations to maintain a constant-anion framework.

Primary clinopyroxene has also been found in this study to be altered to lizardite 1T. According to the calculations and observations of Evans & Trommsdorff (1970), diopside forms a stable assemblage with serpentine (Fig. 9). However, their calculations for this reaction were based on thermochemical data for chrysotile, but their observations were for antigorite of a Type 7 serpentinization. Also, the diopside in equilibrium with the antigorite is of significantly different composition from the primary diopside (Peters 1968), so one could expect the latter to become unstable during serpentinization. The lizardite + secondary diopside pair has not been clearly established for Type 3 serpentinization although diopside is present in rodingites as a product of this serpentinization process.

The veins associated with these textures are composed of lizardite and/or chrysotile (both fibrous and non-fibrous) with or without brucite (Table 3), but the presence of significant amounts of chrysotile asbestos veins can be attributed to process 5.

Type 4. Examples of this are "fish scale" or "fishmeat" serpentine (Cooke 1937) or "Schalenserpentin" (Rost 1959; Klinkhammer 1962; Hochstetter 1965). This is highly sheared, slippery to the touch, slickenside material with a platy texture, which is nevertheless mainly chrysotile with or without lizardite. Some of the material coating the slickensides may be produced by serpentinization elsewhere in the serpentinite and deposited in the shear zones, and some of the serpentine must have formed *in situ*, but it is impossible to distinguish the two. The highly sheared nature of the serpentine makes it difficult to produce thin sections, so that this type does not appear in Table 2, but one example is given in Table 3. Examples described by Coleman (1966, 1971) occur at sheared contact zones or in highly sheared, detached, tectonic serpentinite bodies. Type 4 can only be distinguished from Type 6 by the environment, and not from mineralogical or textural evidence.

Where Type 4 shear zones are adjacent to serpentinite containing pseudomorphic textures of Type 3, the latter is invariably fractured and contains fine veins of chrysotile within the pseudomorphs (Fig. 6b). The material in these veins must represent a volume increase, albeit a small one, and must be derived from the material that

goes into the solution during the topotactic formation of the pseudomorphs.

Type 5. Examples of this are provided in Table 2. Interlocking non-pseudomorphic textures or serrate veins of chrysotile form through the recrystallization of lizardite pseudomorphic textures. At the earliest stages the lizardite pseudomorphs are still recognizable, but chrysotile can be detected, with the microbeam camera, as a component of the pseudomorphs (18500, Pipe Lake mine, Table 1). As recrystallization advances, the pseudomorphs after olivine are rapidly obliterated, but bastites are often slightly more resistant. Relict primary minerals may be altered to crude chrysotile pseudomorphs, often with brucite, which may then be partly obliterated by the developing interlocking textures. Chrysotile asbestos veins associated with non-asbestiform veins of chrysotile, not infrequently of the Povlen-type, or lizardite±brucite commonly form in association with these textures (Table 3).

Spherulitic interlocking textures of multi-layer lizardite may also form in serpentinization of this type, through the recrystallization of lizardite 1T±brucite mesh textures and lizardite 1T bastites, particularly in zones adjacent to multi-layer lizardite veins (Fig. 6a). The development of these more complex polytypes is so closely associated with bastites that their formation might be thought to be due to the release of aluminium from the pyroxenes during serpentinization. However, the aluminium content of many multi-layer lizardites does not seem to be exceptionally high (Wicks 1969).

Type 6. As stated above, this can only be distinguished from Type 4 on environmental grounds. Several examples are listed in Table 3. The Coalinga asbestos deposit (Mumpton & Thompson 1975) is the ultimate example of this type.

Type 7. This is a common process, particularly in regime A of Figure 9, and examples are given in Table 2. Lizardite pseudomorphic textures of Type 3 recrystallize directly to antigorite non-pseudomorphic textures in passing from regime B to A. Relict olivine and chlorite may remain as crude pseudomorphs, but their outlines are blurred or lost during the formation of the antigorite interpenetrating textures. Any veins formed at this stage will be composed of antigorite (Table 3).

The presence of brucite may depend either on its presence in the recrystallizing lizardite texture or on whether regime B or A is reached; however, note also that the conversion of lizardite to

antigorite involves the loss of small amounts of $Mg(OH)_2$ because of the geometry of the inversion lines in the antigorite structure (Zussman 1954; Kunze 1956, 1958, 1961; Whittaker & Wicks 1970). There also may be brucite production by the serpentinization of relict olivine at this stage.

The antigorite+brucite non-pseudomorphic textures (Table 2) form mainly from olivine. This may be the normal path of formation for this particular assemblage. The antigorite grains are generally somewhat less distinct and form interlocking textures in regime B or C, in contrast to the sharply defined blades and interpenetrating textures of the antigorite in regime A.

The antigorite+brucite textures of Type 7 are often associated with chrysotile±brucite textures of Type 5 within the same ultramafic body, and this is usual in asbestos deposits (Jeffrey mine, Tables 1, 2, 3). All form as interlocking or (less frequently) interpenetrating textures, with or without chrysotile and/or antigorite serrate veins (Table 2) and pseudomorphic textures (Table 1), whether through the recrystallization of lizardite±brucite pseudomorphic textures, or through the alteration of primary olivine (or other silicates). Chrysotile asbestos veins commonly form in association with this type, as also do veins of non-fibrous chrysotile and/or lizardite±brucite in regime C and B in Figure 9 (Table 3).

In the lower half of regime A, diopside is stable with antigorite to form an antigorite+diopside±magnetite assemblage (Evans & Trommsdorff 1970), but this assemblage probably only forms through the recrystallization of relict primary assemblages that include diopside (Peters 1968) or tremolite (Trommsdorff & Evans 1974), and would not be formed from a lizardite±brucite pseudomorphic assemblage unless calcium was introduced. If the temperature rises above regime A, amphiboles, talc, and olivine (Wolfe 1967; Trommsdorff & Evans 1972, 1974) are produced at the expense of antigorite.

Type 8. The only example of this type in this work is an antigorite vein sample (Table 3), but this type has been described by Coleman (1966). Type 8 is related to Type 7 in the same way that Type 6 is related to Type 5.

In many cases in all 8 types of serpentinization the veins and rock-forming serpentine are composed of the same mineral, or minerals from the same regime, indicating that the serpentines in the two sites are formed at approximately the same time and approximately in equilibrium. It is also possible for veins to form later, by a type of serpentinization different from that involved

in production of the rock-forming serpentine, and therefore to be out of equilibrium with the host serpentine. For example, chrysotile veins of regime B occur in antigorite interpenetrating textures of regime A (Chidester 1962).

If CO_2 is present in more than minor amounts, the serpentine formed in all types, 1 to 8, of serpentinization will become unstable and will be replaced by talc and carbonates (Naldrett 1966; Greenwood 1967; Johannes 1967).

Magnetite formation and oxidation-reduction processes

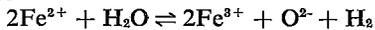
The preceding discussion has been in idealized terms in the sense that it has treated the primary phases as magnesium (±calcium) silicates, whereas in fact they mostly contain substantial amounts of iron replacing magnesium. Some of this iron may enter the serpentine minerals as they form, and there may be concomitant changes of oxidation state. However, because of the relatively low preference for iron in the structures of the serpentine minerals (Whittaker & Wicks 1970) much of the iron goes elsewhere, either into the brucite or to form magnetite, and again redox processes may be involved. These processes also may be involved when conversion of one serpentine mineral into another occurs through recrystallization, since lizardite, chrysotile and antigorite generally have different ferrous:ferric ratios (Whittaker & Wicks 1970; Shteynberg & Chashchukhin 1972; Wicks & Whittaker 1975).

The olivine in ultramafic rocks is commonly about Fe_{90} and the lizardite produced from it in the major serpentinization process (Type 3) contains only about 5 mole % (in round figures) of Fe replacing Mg, mostly as Fe^{3+} . The iron content of brucite may be highly variable but, from the results of Evans & Trommsdorff (1972), an iron component of about 15% would be reasonable for purposes of calculation. The amount of brucite formed is likely to be between 0 and 20% by volume. If the iron that does not enter either lizardite or brucite is assumed to form as magnetite, then we can formulate the reaction in terms of the conversion of 200 oxygen atoms in olivine to 200 oxygen atoms in lizardite+magnetite±brucite as follows:

- i) no brucite formed:
forsterite ($200 O^{2-}$, $90 Mg^{2+}$, $10 Fe^{2+}$) → lizardite ($191 O^{2-}$, $60.2 Mg^{2+}$, $3.1 Fe^{3+}$) + magnetite ($9 O^{2-}$, $2.3 Fe^{2+}$, $4.6 Fe^{3+}$) + solution ($29.8 Mg^{2+}$)
- ii) 20% brucite formed:
forsterite ($200 O^{2-}$, $90 Mg^{2+}$, $10 Fe^{2+}$) → lizardite ($154 O^{2-}$, $48.8 Mg^{2+}$, $2.5 Fe^{3+}$) + brucite ($40 O^{2-}$, $17 Mg^{2+}$ + $3 Fe^{2+}$) + magnetite ($6 O^{2-}$, $1.5 Fe^{2+}$, $3 Fe^{3+}$) + solution ($24.2 Mg^{2+}$)

Thus these extremes respectively require the oxidation of 7.7 and 5.5 of every original 10

Fe^{2+} ions, and this oxidation will clearly be at the expense of water which will be reduced to gaseous hydrogen. This may escape from the system, as has been reported by Thayer (1966). However, the hydrogen will in the process provide a highly mobile reducing medium capable of producing the awaruite and native iron that are observed in minor amounts in serpentinites (Nickel 1959; Chamberlain *et al.* 1965; Ramdohr 1967; Eckstrand 1975). Therefore, the existence of these phases does not imply reducing conditions, as such, during serpentinization, but is a function of the lower oxidation potential of Fe^{3+} in the lizardite and magnetite structures than in the olivine structure, which permits the reaction



to move towards the right. That the iron is a highly mobile element between the various mineral phases and the solution is indicated by the behavior of the magnetite that is formed. Magnetite initially forms as small discrete grains within the textural units, but migrates during pervasive serpentinization to form coarser grains and stringers still within the textural units, and finally to form even coarser cross-cutting lenses and veins which cut through the textural units. In a parallel development, the chemical composition of all the minerals becomes fairly uniform among the various textural units (Wicks 1969; Wicks & Plant 1972). Because the iron that is rejected by the lizardite probably has to go either into brucite or into magnetite, any factors that limit the oxidation of iron will increase the quantity (and iron content) of brucite. This is in line with the observed indication of an antipathetic variation in amounts of brucite and magnetite.

The formation of bastites (mainly from orthopyroxene) in Type 3 serpentinization differs from the formation of mesh texture from olivine in that, although the pyroxene contains a similar Fe:Mg ratio, very little magnetite is formed. This is presumably because there is no excess of cations to be disposed of [the ratio (Mg+Fe):O = 1:3 in both enstatite and lizardite, Table 5], and magnetite can only be formed if some compensating magnesium is carried into the bastite from surrounding olivine. There is, in fact, evidence for a higher iron content in the lizardite of bastites than in mesh textures (Page 1967a, 1968; Wicks & Plant 1972) as would be expected for this reason.

Because chrysotile has lower total iron than lizardite, its direct formation in Type 4 serpentinization, and in Types 5 and 6 serpentinization of relict minerals, leads to a greater rejection of iron and to the production of a smaller amount

of hydrogen. Since antigorite has lower ferric iron than lizardite, its formation in Types 1 and 2 serpentinization, and in Types 7 and 8 serpentinization of relict minerals, will also lead to similarly reduced hydrogen production. On the other hand, when lizardite recrystallizes to antigorite in processes of Types 7 and 8, some reduction of ferric iron will usually occur, and this is probably also true to a lesser extent for recrystallization to chrysotile in Types 5 and 6. This process will raise the oxygen fugacity of the aqueous phase and, in the presence of carbon dioxide, may be responsible for the conversion of brucite to frequently observed pyroaurite, brugnatellite, and similar minerals. Whether these minerals are constituents of the serpentinites, or whether they have been produced by subsequent oxidative carbonation, is uncertain.

CHRYSOTILE ASBESTOS DEPOSITS

Chrysotile asbestos deposits are characterized by a specific association of textures (Grubb 1962). These textures have been studied in more detail and can be further interpreted in terms of the classification of serpentinization processes that we have advanced. In the host rock of these deposits, lizardite 17 mesh textures with lizardite or unaltered olivine centers are rare, whereas the corresponding pure hourglass textures are common and are frequently associated with, and recrystallized to, non-pseudomorphic interlocking textures of antigorite+brucite, chrysotile±brucite, and chrysotile+lizardite±brucite. This suggests that asbestos deposits are confined to serpentinites formed under special conditions of metamorphism, in addition to being confined to the structural conditions needed to open the fractures and shears in which the asbestos fibers are able to grow, and to the appropriate mineralogy needed to provide the material required for the formation of the asbestos veins, as discussed in Table 5. Normal Type 3 serpentinization is involved, but either it goes to completion (giving the pure hourglass textures) and is followed by processes of Type 5 or 7, to the upper limit of regime B, or it is interrupted by these processes so that there is no time at which lizardite mesh centers can arise. The formation of asbestos deposits then further requires that the rising temperature does not reach regime A of Figure 9, where chrysotile asbestos would be unable to form, and that the appropriate fracturing of the rock provides a site for asbestos growth at the same time. The importance of shearing (Type 6 serpentinization) was recognized by Rost (1949, 1959) and reaches its ultimate expression in the Coalinga deposit described by Mumpton &

Thompson (1975). The recognition of this specific association of textural characteristics could be of importance in the exploration for asbestos deposits, since it presents a further criterion for evaluating possible formations, and could provide a basis for exploration programs.

The Manitoba Nickel Belt serpentinites examined in this study form an interesting example of trends which may be found in studies of this kind, and which may be relevant in exploration. At the southwestern end of the belt, Little Clarke Lake and Bucko Lake (18494, 18495, 18492, Table 1) serpentinitized ultramafic bodies are composed of lizardite mesh textures. However, towards the northeast, at Bowden and Setting lakes, non-pseudomorphic lizardite interlocking textures occur which contain lizardite veins with the same texture (18503, Table 2). Farther northeast, lizardite hourglass textures occur at Joey Lake (18493, Table 1); slightly farther northeast at Pipe Lake mine, lizardite mesh and hourglass textures have been recrystallized to chrysotile+lizardite interlocking textures and chrysotile+lizardite mesh textures (18499, 18500, 18501, Table 1). Here, chrysotile asbestos veins are abundant, although the Pipe Lake mine is a nickel mine, not an asbestos mine. These limited textural studies seem to indicate, in a very general way, that conditions for the formation of asbestos become increasingly favorable from the southwest towards the northeast.

ACKNOWLEDGEMENTS

Thanks are especially due to Prof. J. Zussman, Manchester University, for initiating the present approach to the problem of serpentine textures, and for much help and guidance in the earlier stages of the work, from which the present discussion grew. Many of our ideas were developed through discussion and debate with Dr. R. F. J. Scoates, Manitoba Mines Branch and Dr. C. J. A. Coats, Falconbridge Nickel Mines Ltd., to whom our appreciation is extended.

Some of the samples were collected by one of us (FJW) and others were supplied by those listed. Our thanks are extended to all those who responded to our requests: Prof. F. Aumento, Halifax; Dr. B. B. Bannatyne, Manitoba Mines Branch, Winnipeg; Prof. G. M. Brown, Durham; Dr. J. J. Brummer, Occidental Mineral Corp., Toronto; Mr. R. M. Buchanan, CANMET, Ottawa; Dr. C. J. A. Coats, Falconbridge Nickel Mines Ltd., Winnipeg; Prof. I. G. Gass, The Open University; the late Prof. H. H. Hess, Princeton; Dr. R. Hutchison, British Museum; Dr. T. N. Irvine, Geophysical Laboratory, Wash-

ington; Dr. F. Machado, Lab. Est. Petrologicas e Paleontologicas do Ultramar, Lisbon; Dr. L. J. Monkman, Turner and Newall Asbestos Fibre Lab., Manchester; Dr. E. R. Oxburgh, Oxford; Dr. B. Windley, Leicester; Prof. J. Zussman, Manchester.

We are grateful to Falconbridge Nickel Mines Ltd. and Canadian Johns-Manville Co. Ltd. for allowing one of us (FJW) access to their properties. Our thanks are due to Miss Helen Driver and Ms. Mary Nix, Royal Ontario Museum, who carefully typed the lengthy manuscript and to Mrs. Joey Galt, Royal Ontario Museum, who patiently typed the tables.

REFERENCES

- ANGEL, F. (1930): Stubachit und Stubachitserpentin vom Ganoz (Bei Kals in Osttril). *Z. Krist.* **72**, 1-41.
- (1964): Petrographische Studie an der Ultramafit-Masse von Kraubath (Steiermark). *Joanneum Mineral. Mitt.* **2**, 1-123.
- AUMENTO, F. (1970): Serpentine mineralogy and ultrabasic intrusions in Canada and on the Mid-Atlantic Ridge. *Geol. Surv. Can. Pap.* **69-53**.
- BARNES, I. & O'NEIL, J. R. (1969): The relationship between fluids in some fresh alpine-type ultramafics and possible modern serpentinization, western United States. *Geol. Soc. Amer. Bull.* **80**, 1947-1960.
- , RAPP, J. B., O'NEIL, J. R., SHEPPARD, R. A. & GUDE, A. J. (1972): Metamorphic assemblages and the direction of flow of metamorphic fluids in four instances of serpentinization. *Contr. Mineral. Petrology* **35**, 263-276.
- BOUDIER, F. (1971): Minéraux serpentiniteux extraits de péridotites serpentinisées des Alpes Occidentales. *Contr. Mineral. Petrology* **33**, 331-345.
- BUCHER, K. & PFEIFER, H. R. (1973): Über Metamorphose und Deformation der östlichen Malenco-Ultramafite und deren Rahmengesteine (Prov. Sondrio, N-Italien). *Schweiz. Mineral. Petrol. Mitt.* **53**, 231-242.
- CHAMBERLAIN, J. A., McLEOD, C. R., TRAILL, R. J. & LACHANCE, G. R. (1965): Native metals in the Muskox Intrusion. *Can. J. Earth Sci.* **2**, 188-215.
- CHERNOSKY, J. V. (1971): Minerals of the serpentine group. *Carnegie Inst. Wash. Year Book* **70**, 153-157.
- (1975): Aggregate refractive indices and unit cell parameters of synthetic serpentine in the system $MgO-Al_2O_3-SiO_2-H_2O$. *Amer. Mineral.* **60**, 200-208.
- CHIDESTER, A. H. (1962): Petrology and geochemistry of selected talc-bearing ultramafic rocks and adjacent country rocks in north-central Vermont. *U.S. Geol. Surv. Prof. Pap.* **345**, 1-207.

- CLARK, A. L. & GREENWOOD, W. R. (1972): Petrographic evidence of volume increase related to serpentinization, Union Bay, Alaska. *U.S. Geol. Surv. Prof. Pap.* 800-C, 21-27.
- COLEMAN, R. G. (1966): New Zealand serpentinites and associated metasomatic rocks. *New Zealand Geol. Surv. Bull.* N.S. 76.
- (1971): Petrologic and geophysical nature of serpentinites. *Geol. Soc. Amer. Bull.* 82, 897-918.
- & KEITH, T. E. (1971): A chemical study of serpentinization — Burro Mountain, California. *J. Petrology* 12, 311-328.
- COOKE, H. C. (1937): Thetford, Disraeli and eastern half of Warwick map areas, Quebec. *Geol. Surv. Can. Mem.* 211.
- CRESSEY, B. A. & ZUSSMAN, J. (1976): Electron microscope studies of serpentinite. *Can. Mineral.* 14, 307-313.
- DIETRICH, V. & PETERS, T.J. (1971): Regionale Verteilung der Mg-Phyllosilikate in den Serpentiniten des Oberhalbsteins. *Schweiz. Mineral. Petrog. Mitt.* 51, 329-348.
- DUNGAN, M. A. (1977): Metastability in serpentine-olivine equilibria. *Amer. Mineral.* 62, 000-000.
- DU RIETZ, T. (1935): Peridotite, serpentines and soapstones of northern Sweden. *Geol. Fören. Stockholm Förh.* 57, 133-260.
- ECKSTRAND, O. R. (1975): The Dumont serpentinite: a model for control of nickeliferous opaque mineral assemblages by alteration reactions in ultramafic rocks. *Econ. Geol.* 70, 183-201.
- EVANS, B. W. & TROMMSDORFF, V. (1970): Regional metamorphism of ultramafic rocks in the central Alps: Paragenesis in the system CaO-MgO-SiO₂-H₂O. *Schweiz. Mineral. Petrog. Mitt.* 50, 481-492.
- & —— (1972): Einfluss des Eisens auf die Hydratisierung von Duniten. *Schweiz. Mineral. Petrog. Mitt.* 52, 251-256.
- , Johannes, W., Oterdoom, H. & Trommsdorff, V. (1976): Stability of chrysotile and antigorite in the serpentine multisystem. *Schweiz. Mineral. Petrog. Mitt.* 56, 79-93.
- FAUST, G. T. & FAHEY, J. J. (1962): The serpentine group minerals. *U.S. Geol. Surv. Prof. Pap.* 384A, 1-92.
- FLETT, J. S. (1946): Geology of the Lizard and Meneage (explanation of sheet 359). *Mem. Geol. Surv. Gt. Brit.*
- FRANCIS, G. H. (1956): The serpentinite mass in Glen Urquhart, Inverness-shire, Scotland. *Amer. J. Sci.* 254, 201-226.
- GEES, R. A. (1956): Ein Beitrag zum Ophiolith-Problem behandelt ein einigen Beispielen aus dem Gebiet von Klosters-Davos (Graubünden). *Schweiz. Mineral. Petrog. Mitt.* 36, 454-488.
- GILLERY, F. H. (1959): The X-ray study of synthetic Mg-Al serpentines and chlorites. *Amer. Mineral.* 44, 143-152.
- GREEN, D. H. (1961): Ultramafic breccias from the Musa Valley, eastern Papua. *Geol. Mag.* 98, 1-26.
- GREENWOOD, H. J. (1967): Mineral equilibria in the system MgO-SiO₂-H₂O-CO₂. In *Researches in Geochemistry 2* (P. H. Abelson, ed.). John Wiley & Sons, N.Y., 542-567.
- GRESENS, R. L. (1967): Composition-volume relationships of metasomatism. *Chem. Geol.* 2, 47-65.
- (1969): Blueschist alteration during serpentinization. *Contr. Mineral. Petrology* 24, 93-113.
- GRUBB, P. L. C. (1962): Serpentinization and chrysotile formation in the Matheson ultrabasic belt, northern Ontario. *Econ. Geol.* 57, 1228-1246.
- HAHN-WEINHEIMER, P. & ROST, F. (1961): Akzessorische Mineralien und Elemente im Serpentin von Leupoldsgrün (Münchberger Gneismasse). Ein Beitrag zur Geochemie ultrabasischer Gesteine. *Geochim. Cosmochim. Acta.* 21, 165-181.
- HADINGER, W. (1845): *Naturwissenschaftliche Abhandlungen*. Vols. 1-4. Wien.
- HAUSMANN, J. F. L. (1808): *Moll's Efemeriden der Berg und Huttenkunde*. Vol. 4, 401.
- HEMLEY, J. J., MONTOYA, J. W., CHRIST, C. L. & HOSTETLER, P. B. (1977): Mineral equilibria in the MgO-SiO₂-H₂O system: I talc-chrysotile-forsterite-brucite stability relations. *Amer. J. Sci.* 277, 322-351.
- , ——, SHAW, D. R. & LUCE, R. W. (1977): Mineral equilibria in the MgO-SiO₂-H₂O system: II talc-antigorite-forsterite-anthophyllite-enstatite stability relations and some geologic implications in the system. *Amer. J. Sci.* 277, 353-383.
- HESS, H. H., SMITH, R. J. & DENG, G. (1952): Antigorite from the vicinity of Caracas, Venezuela. *Amer. Mineral.* 37, 68-75.
- HOCHSTETTER, R. (1965): *Zur Kenntnis der Serpentinmineralien*. Ph.D. thesis, Univ. des Saarlandes.
- HOSTETLER, P. B., COLEMAN, R. G., MUMPTON, F. A. & EVANS, B. W. (1966): Brucite in alpine serpentinites. *Amer. Mineral.* 51, 75-98.
- ISHI, K. & SAITO, M. (1973): Synthesis of antigorite. *Amer. Mineral.* 58, 915-919.
- JASMUND, K. & SYLLA, H. M. (1971): Synthesis of Mg- and Ni- antigorite. *Contr. Mineral. Petrology* 34, 84-86.
- & —— (1972): Synthesis of Mg- and Ni-antigorite: a correction. *Contr. Mineral. Petrology* 34, 346.
- JOHANNES, W. (1967): Zur Bildung und Stabilität von Forsterit, Talk, Serpentin, Quarz und Magnetit im System MgO-SiO₂-H₂O-CO₂. *Contr. Mineral. Petrology* 15, 233-250.

- (1968): Experimental investigation of the reaction forsterite + $H_2O \rightleftharpoons$ serpentinite + brucite. *Contr. Mineral. Petrology* 19, 309-315.
- (1975): Zur Synthese und thermischen Stabilität von Antigorit. *Fortschr. Mineral.* 53, 36.
- KEUSEN, H. R. (1972): Mineralogie und Petrographie des metamorphen Ultramafitit-Komplexes vom Geisspfad (Penninische Alpen). *Schweiz. Mineral. Petrog. Mitt.* 52, 385-478.
- KING, E. G., VARANY, R., WELLER, W. W. & PANKRAZ, L. B. (1967): Thermodynamic properties of forsterite and serpentinite. *U.S. Bur. Mines Rep. Invest.* 6962.
- KLINKHAMMER, B. F. (1962): *Ultrabasite des Ostbayerischen Grenzgebirges*. Ph.D. thesis, Univ. des Saarlandes.
- & ROST, F. (1967): Die Serpentinite des Oberpfälzer Waldes. *Zur Mineral. Geol. Oberpfalz* 16, 112-136.
- KORYTKOVA, E. N. & MAKAROVA, T. A. (1971): Experimental study of the serpentinization of olivine. *Dokl. Akad. Nauk U.S.S.R.* 196, 144-145.
- , KOSALINA, G. I. & MAKAROVA, T. A. (1972): Experimental serpentinization of olivine. *Int. Geol. Rev.* 14, 1074-1078.
- KRSTANOVIĆ, I. & PAVLOVIĆ, S. (1964): X-ray study of chrysotile. *Amer. Mineral.* 49, 1769-1771.
- KUNZE, G. (1956): Die gewellte Struktur des Antigorits. *I. Z. Krist.* 108, 82-107.
- (1958): Die gewellte Struktur des Antigorits. *II. Z. Krist.* 110, 282-320.
- (1961): Antigorit. Strukturtheoretische Grundlagen und ihre praktische Bedeutung für die weitere Serpentin-Forschung. *Fortschr. Mineral.* 39, 206-324.
- LAPHAM, D. M. (1964): Spinel-orthopyroxene compositions and their bearing upon the origin of the serpentinite near Mayaguez, Puerto Rico. *NAS-NRC Publ.* 1188, 134-144.
- LEECH, G. B. (1953): Geology and mineral deposits of the Shulaps range, southwestern British Columbia. *B. C. Dept. Mines Bull.* 32.
- LODOCHNIKOV, W. N. (1933): Serpentinates and serpentinites and the petrological problems connected with them. *Problems Soviet Geol.* 2, 145-150.
- MAGARITZ, M. & TAYLOR, H. P. (1974): Oxygen and hydrogen isotope studies of serpentinization in the Troodos complex, Cyprus. *Earth Planet. Sci. Letters* 23, 8-14.
- MARTIN, B. (1971): Some comments on the process of serpentinization from experimental and other work. *Geol. Soc. Australia Spec. Publ.* 3, 301-310.
- & FYFE, W. S. (1970): Some experimental and theoretical observations on the kinetics of hydration reactions with particular reference to serpentinization. *Chem. Geol.* 6, 185-202.
- MATTSON, P. H. (1964): Petrography and structure of serpentinite from Mayaguez, Puerto Rico. *NAS-NRC Publ.* 1188, 7-24.
- MERENKO, B. YA. (1958): The genesis of chrysotile asbestos. *Trans. Acad. Sci. U.S.S.R.* 22, (Trans. by Geol. Surv. Can.).
- MIDDLETON, A. P. & WHITTAKER, E. J. W. (1976): The structure of Povlen-type chrysotile. *Can. Mineral.* 14, 301-306.
- MOODY, J. B. (1976): An experimental study on the serpentinization of iron-bearing olivines. *Can. Mineral.* 14, 462-478.
- MUMPTON, F. A. & THOMPSON, C. S. (1975): Mineralogy and origin of the Coalinga asbestos deposit. *Clays Clay Minerals* 23, 131-143.
- NALDRETT, A. J. (1966): Talc-carbonate alteration of some serpentinized ultramafic rocks south of Timmins, Ontario. *J. Petrology* 7, 489-499.
- NICKEL, E. H. (1959): The occurrence of native nickel-iron in the serpentine rock of the Eastern Townships of Quebec Province. *Can. Mineral.* 6, 307-319.
- NICOLAS, A. (1967): Géologie des Alpes piémontaises entre Dora Maria et Grand Paradis. *Trav. Lab. Geol. Grenoble* 43, 139-167.
- (1969): Tectonique et métamorphisme dans les Stura di Lanzo (Alpes Piémontaises). *Bull. Suisse Mineral. Petrog.* 49, 359-377.
- O'HARA, M. J. (1967): Mineral facies in ultrabasic rocks. In *Ultramafic and Related Rocks* (P. J. Wyllie, ed.), John Wiley & Sons, N.Y., 7-18.
- OLSEN, E. J. (1963): Equilibrium calculations in the system Mg, Fe, Si, O, H, and Ni. *Amer. J. Sci.* 261, 943-956.
- O'NEIL, J. R. & BARNES, I. (1971): C^{13} and O^{18} compositions in some fresh-water carbonates associated with ultramafic rocks and serpentinites: western United States. *Geochim. Cosmochim. Acta* 35, 687-697.
- PAGE, N. J. (1967a): Serpentinization at Burro Mountain, California. *Contr. Mineral. Petrology* 14, 321-342.
- (1967b): Serpentinization considered as a constant volume metasomatic process: a discussion. *Amer. Mineral.* 52, 545-549.
- (1968): Serpentinization in a sheared serpentinite lens, Tiburon Peninsula, California. *U.S. Geol. Surv. Prof. Pap.* 600-B, 21-28.
- (1976): Serpentinization and alteration in a olivine cumulate from the Stillwater Complex, southwestern Montana. *Contr. Mineral. Petrology* 54, 127-137.
- PETERS, T.J. (1963): Mineralogie und Petrographie des Totalserpentin bei Davos. *Schweiz. Mineral. Petrog. Mitt.* 43, 529-685.
- (1968): Distribution of Mg, Fe, Al, Ca and Na in coexisting olivine orthopyroxene and clinopyroxene in the Totalp serpentinite (Davos, Switzerland) and in the alpine metamorphosed Malenco serpentinite (N. Italy). *Contr. Mineral. Petrology* 18, 65-75.

- RAMDOHR, P. (1967): A widespread mineral association, connected with serpentinization. *Neues Jahrb. Mineral. Monatsh.* 107, 241-265.
- RIORDON, P. H. (1955): The genesis of asbestos in ultrabasic rocks. *Econ. Geol.* 50, 67-81.
- ROST, F. (1949): Das Serpentin-Gabbro-Volkommen von Wurlitz und seine Mineralien. *Heidelberg. Beitr.* 1, 626-688.
- (1959): Probleme ultrabasischer Gesteine und ihrer Lagerstätten. *Freiberger Forsch.* C58, 28-65.
- (1961): Chlorit und Granat in ultrabasischen Gesteinen. *Fortschr. Mineral.* 39, 112-126.
- ROY, D. M. & ROY, R. (1954): An experimental study of the formation and properties of synthetic serpentines and related layer silicate minerals. *Amer. Mineral.* 39, 959-975.
- SCARFE, C. M. & WYLLIE, P. J. (1967): Serpentine dehydration curves and their bearing on serpentine deformation in orogenesis. *Nature* 215, 945-946.
- SELFRIDGE, G. C. (1936): An X-ray and optical investigation of the serpentine minerals. *Amer. Mineral.* 21, 463-503.
- SHTENBERG, D. S. & CHASHCHUKHIN, I. S. (1972): Behavior of trivalent iron in serpentinization. *Int. Geol. Rev.* 14, 495-504.
- SMITH, C. H. (1958): Bay of Islands Igneous Complex, western Newfoundland. *Geol. Surv. Can. Mem.* 290.
- THAYER, T. P. (1966): Serpentinization considered as a constant-volume metasomatic process. *Amer. Mineral.* 51, 685-710.
- (1967): Serpentinization considered as a constant volume metasomatic process: a reply. *Amer. Mineral.* 52, 549-553.
- THOMPSON, R. B. (1968): Serpentinization accompanied by volume changes. *Pacific Geol.* 1, 167-174.
- TRÖGER, W. E. (1969): *Optische Bestimmung der gesteinsbildenden Minerale* 2. E. Schweizerbart, Stuttgart.
- TROMMSDORFF, V. & EVANS, B. W. (1972): Progressive metamorphism of antigorite schist in the Bergell tonalite aureole (Italy). *Amer. J. Sci.* 272, 423-437.
- & ——— (1974): Alpine metamorphism of peridotitic rocks. *Schweiz. Mineral. Petrog. Mitt.* 54, 333-352.
- VANCE, J. A. & DUNGAN, M. A. (1977): Formation of peridotites by deserpentinization in the Darrington area, Cascade Mountains, Washington. *Geol. Soc. Amer. Bull.* 88, 000-000.
- VARLAKOV, A. S. (1975): Stubachite, a special kind of dunite in alpine-type harzburgite massifs. *Int. Geol. Rev.* 16, 1205-1213.
- WEIGAND, B. (1875): Die Serpentine der Vogesen. *Tschermaks Mineral. Petrog. Mitt.* 3, 183-206.
- WENNER, D. B. & TAYLOR, H. P. JR. (1971): Temperatures of serpentinization of ultramafic rocks based on O^{18}/O^{16} fractionation between coexisting serpentine and magnetite. *Contr. Mineral. Petrology* 32, 165-185.
- & ——— (1973): Oxygen and hydrogen isotope studies of the serpentinization of the ultramafic rocks in oceanic environments and continental ophiolite complexes. *Amer. J. Sci.* 273, 207-239.
- & ——— (1974): O/H and O^{18}/O^{16} studies of serpentinization of ultramafic rock. *Geochim. Cosmochim. Acta* 38, 1255-1286.
- WHITTAKER, E. J. W. & WICKS, F. J. (1970): Chemical differences among the "serpentine" "polymorphs": a discussion. *Amer. Mineral.* 55, 1025-1047.
- & ZUSSMAN, J. (1956): The characterization of serpentine minerals by X-ray diffraction. *Mineral. Mag.* 31, 107-126.
- WICKS, F. J. (1969): *X-ray and Optical Studies on Serpentine Minerals*. D. Phil. thesis, Oxford Univ.
- & PLANT, A. G. (1972): Some electron microprobe observations on serpentine minerals. *Can. Mineral.* 11, 581-582 (Abstr.).
- & WHITTAKER, E. J. W. (1975): A reappraisal of the structures of the serpentine minerals. *Can. Mineral.* 13, 227-243.
- & ZUSSMAN, J. (1975): Microbeam X-ray diffraction patterns of the serpentine minerals. *Can. Mineral.* 13, 244-258.
- , WHITTAKER, E. J. W. & ZUSSMAN, J. (1977): An idealized model for serpentine textures after olivine. *Can. Mineral.* 15, 000-000.
- WINCHELL, A. N. & WINCHELL, H. (1959): *Elements of Optical Mineralogy*. Part II, 4th ed. John Wiley & Sons, N.Y.
- WOLFE, W. J. (1967): *Petrology, Mineralogy and Geochemistry of the Blue River Ultramafic Intrusion, Cassiar District, British Columbia*. Ph.D. thesis, Yale Univ.
- YODER, H. S. (1952): The $MgO-Al_2O_3-SiO_2-H_2O$ system and related metamorphic facies. *Amer. J. Sci.* Bowen Vol. 569-627.
- ZUSSMAN, J. (1954): Investigation of the crystal structure of antigorite. *Mineral. Mag.* 30, 498-512.

Received April 1977; revised manuscript accepted July 1977.